Hindawi
Mathematical Problems in Engineering
Volume 2022, Article ID 6929776, 28 pages
https://doi.org/10.1155/2022/6929776

Research Article

Simulation and Experimental Investigations on the Sugarcane Cutting Mechanism and Effects of Influence Factors on the Cutting Quality of Small Sugarcane Harvesters under Vibration Excitations

Hanning Mo,[1,2] **Shangping Li**,[3] **Jinghui Zhou**,[4] **Bang Zeng**,[5] **Guiqing He**,[5] **and Chen Qiu**[2]

[1]*College of Light Industry and Food Engineering, Guangxi University, Nanning 530004, China*
[2]*School of Mechanical and Material Engineering, Wuzhou University, Wuzhou 543000, China*
[3]*College of Electronic Information, Guangxi University for Nationalities, Nanning 530006, China*
[4]*Department of Mechanical and Control Engineering, Guilin University of Technology at Nanning, Nanning 532100, China*
[5]*School of Mechanical Engineering, Guangxi University, Nanning 530004, China*

Correspondence should be addressed to Shangping Li; spli501@vip.sina.com

Received 4 October 2021; Revised 2 December 2021; Accepted 18 December 2021; Published 31 January 2022

Academic Editor: Goutam Pohit

Copyright © 2022 Hanning Mo et al. This is an open access article distributed under the Creative Commons Attribution License, which permits unrestricted use, distribution, and reproduction in any medium, provided the original work is properly cited.

In order to study the sugarcane cutting mechanism and the effects of influence factors on the sugarcane cutting quality (SCQ) of small sugarcane harvesters in hilly areas, sugarcane cutting experiments and simulations were done through a self-developed sugarcane harvester experiment platform (SHEP) and the finite element analysis (FEA) method. The comprehensive cutting quality evaluating value (CCQEV) was calculated through the number of sugarcane cracks, the crack thickness, and the crack length to evaluate the SCQ. Effects of the amplitude and the frequency of the axial cutter vibration, the cutter rotation velocity, the sugarcane feeding velocity, and the cutter installing angle on the CCQEV were studied. Effects of interaction between the amplitude and the frequency of the axial cutter vibration and that between the axial cutter vibration amplitude and the cutter rotation velocity on the CCQEV were also studied. The sugarcane cutting mechanism was studied through analysis of cutting force signals, the high-speed photographing result in the sugarcane cutting process, and FEA simulations of the sugarcane cutting process, which verified discoveries obtained through sugarcane cutting experiments. This research laid the foundation for the development of small sugarcane harvesters with a good SCQ in hilly areas.

1. Introduction

The mechanized sugarcane harvesting area is only 5% of the whole planting area [1]. A very important reason for difficult mechanized sugarcane harvesting promotion is that it brings a poor sugarcane cutting quality. The poor sugarcane cutting quality causes ratoons to be broken and affects the ratoon budding rate of the subsequent year.

Aimed at the poor cutting quality of mechanized sugarcane harvesting, related research was done by scholars all over the world. Kroes [2, 3] and Mello [4] studied the effects of cutting forces, cutting energies, and different cutting edge positions on the sugarcane cutting quality through experiments. Kroes [5] studied the effects of sugarcane-pressing rollers, cutters, the cutter installing angle, and the distance among saw teeth of cutting edges on the sugarcane cutting quality through simulations. Mello and Harris [6] studied the effect of penetrating cutting on the sugarcane cutting quality. Liu et al. [7, 8] studied the broken forms of sugarcanes suffering from tensions, compressions, bending and torsional moments, and kinematics of sugarcanes cut by plain knives. Liu et al. [9] explored the cutting mechanism and mechanical

properties of the sugarcane stem material. Yang Jian [10] studied the effects of sugarcane fields and machine structural factors on the sugarcane ratoon breaking rate. Yang Wang [11] studied the sugarcane cutting mechanism through an emulator of the sugarcane-cutter system with changeable structural and kinematic parameters, laying a theoretical foundation of sugarcane cutting quality improvement.

Moreover, Thanomputra used the high-pressure water cutting method with abrasive sands added to improve the sugarcane cutting efficiency [12]. Mello [13] and Momin [14] used different blades to carry on experimental research on the sugarcane cutting quality and they found that bending-angle-shape blades with or without saw teeth can improve the sugarcane cutting quality. Ripoli designed a cutter whose cutting depth into soils can be adjusted according to the gradient variation of sugarcane fields [15]. This cutter reduced the sugarcane wastage and the impurity content. Johnson et al. [16] and Mathanker et al. [17] studied the effects of the cutting velocity and the cutting edge angle on the cutting energy. Kroes designed a double-cutter model to study the kinematic trajectory of the cutters and calculated the maximum velocity ratio between the sugarcane harvester moving velocity and the cutter rotation velocity to improve the cutting quality [18]. Kroes measured forces and the bending strength of sugarcane ratoons during the cutting process [19]. Silva evaluated the sugarcane root damage degree caused by cut-in height differences through experiments [20]. Lai Xiao found that the sugarcane field excitation has effects on the cutting system of sugarcane harvesters, causes the vertical cutter frame vibration, and deteriorates the sugarcane cutting quality [21, 22]. Wang and Wei designed a cutter vibration model to study the effect of the bearing clearance on the cutting system vibration [23]. Huang et al. used ANSYS/LS-DYNA to simulate the sugarcane cutting process through the infinite element method and found that the cutting force is the minimum when the cutter installing angle is 0° and the greater the cutting velocity is, the greater the cutting force will be [24]. Liu et al. studied relationships among the sliding cutting angle, the cutter installing angle, the cutting velocity, and the cutting force through experiments [25]. Xu et al. designed a cutting system model and obtained cutting force curves and displacement cloud pictures during the cutting process through simulations [26]. Yang et al. [27] and Pelloso et al. [28] studied the effects of the cutter rotation velocity and the sugarcane harvester moving velocity on the cutting quality.

The research mentioned above was focused on the effects of sugarcane cutting form, cutter parameters, cutting system vibration, sugarcane harvester moving velocity, and cutter rotation velocity on the sugarcane cutting quality and cutting forces. However, none of the research mentioned above was focused on the effect of the axial cutter vibration on the sugarcane cutting quality. It is indicated through experiments done by our research group that the axial cutter vibration has a bad effect on the sugarcane cutting quality [29]. The word "axial" means the direction along the cutter axis when the cutter installing angle is 0°. Furthermore, none of the research mentioned above was focused on how three-directional cutting forces and stresses acting on sugarcanes change during the cutting process. Therefore, it is necessary to do further research on the effects of the axial cutter vibration and relative factors on the sugarcane cutting quality and the cutting mechanism.

In previous research of our research group, eccentric mass blocks installed on the cutters of a sugarcane harvester experiment platform (SHEP) developed by our research group were used to simulate the axial cutter vibration caused by the sugarcane field excitation and control the axial cutter vibration displacement and frequency. Under vibration excitations simulated by eccentric mass blocks and cutting forces, effects of the axial cutter vibration amplitude, the cutter rotation velocity, and the sugarcane harvester moving velocity on the sugarcane cutting quality were studied. It is found that significance levels of effects of these factors on the sugarcane cutting quality from high to low are as follows: the axial cutter vibration amplitude, the unbalanced mass, the cutter rotation velocity, and the sugarcane harvester moving velocity [30]. However, when the axial cutter vibration caused by the sugarcane field excitation were simulated through eccentric mass blocks installed on cutters of the SHEP, the effect of the axial cutter vibration frequency on the sugarcane cutting quality could not be studied. Besides, the effect of the cutter installing angle on the sugarcane cutting quality has not been studied yet.

In this paper, sugarcane cutting experiments were done on the SHEP to study effects of the amplitude and the frequency of the axial cutter vibration and related cutting parameters on the cutting quality of small sugarcane harvesters in hilly areas. Simulations of the sugarcane cutting process were done to study the sugarcane cutting mechanism.

2. Design Analysis on the SHEP

The manufactured SHEP and its structural diagram are shown in Figure 1. It is mainly composed of a sugarcane-clamping device, a sugarcane-feeding device, a sugarcane-feeding pathway (SFP), a cutting system, and eccentric vibration devices. A variable-frequency velocity-adjusting motor (Model: JB/T8680-2008) was used to control the moving velocity and direction of the sugarcane-feeding device along the SFP, which simulates the sugarcane harvester moving velocity. Sugarcanes were placed in the sugarcane-clamping device and driven by the sugarcane-feeding device to move along the SFP. The sugarcane-clamping device has 9 sockets. A sugarcane was inserted into a socket and fixed by 8 springs to imitate the tightening effect of soils. Therefore, 9 sugarcanes can be cut every time. Two cutters consist of 2 disks both with a diameter of 450 mm and are connected with four blades of 80 mm length and 5 mm thickness; they are driven by a stepless velocity-adjusting hydraulic motor (Model: CM-FM40-FL. The rotation velocity adjusting range: 120 RPM–2400 RPM) and a reverse magnetic value is used to make them positively and negatively rotate. The eccentric vibration device is used to make the SFP repeatedly swing around the fixed hinged support, which can generate axial vibrations at sugarcane cutting points to stimulate axial vibrations generated by cutters and sugarcane harvesters under the sugarcane field excitation. Sugarcane cutting points are

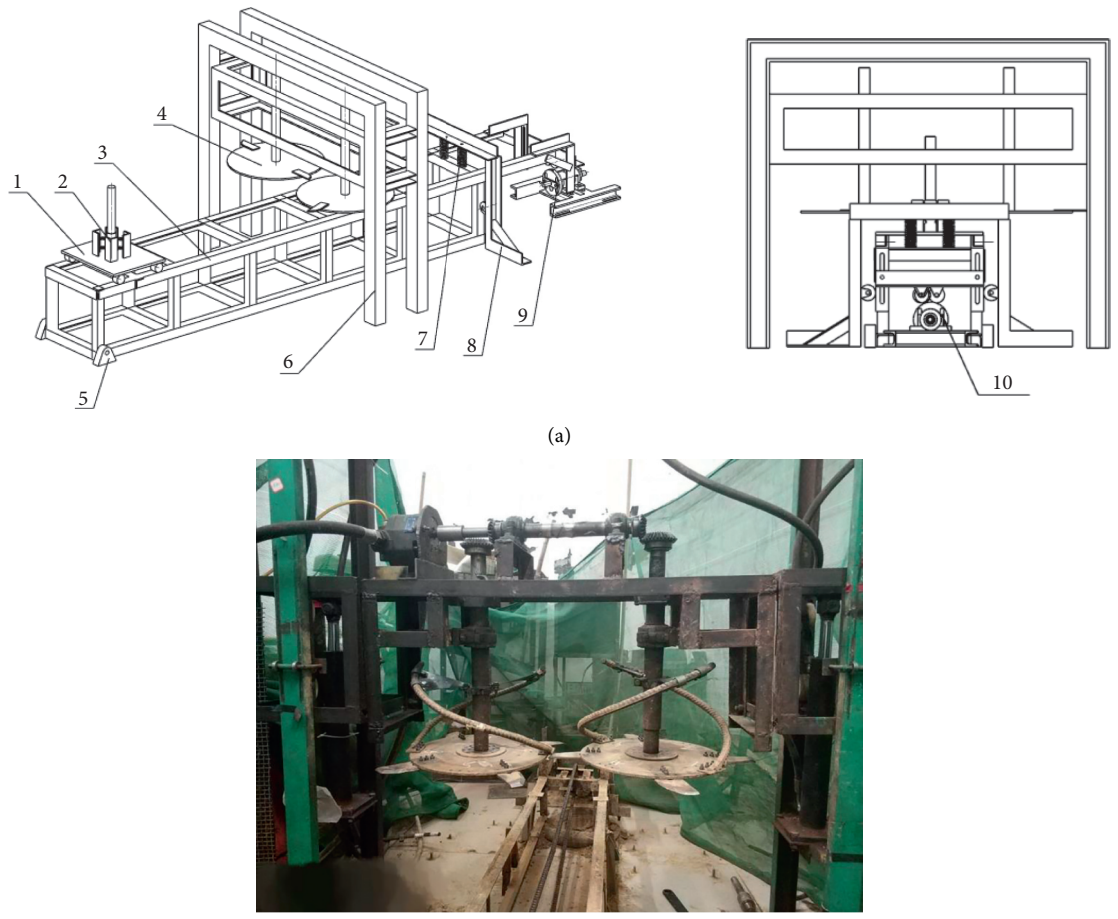

Figure 1: The SHEP. (a) The structural diagram of the SHEP. (b) The manufactured SHEP. (1) The sugarcane-feeding device. (2) The sugarcane-clamping device. (3) The SFP. (4) The cutter with two blades. (5) The fixed hinged support of the SFP. (6) The cutter holder. (7) The hold-down spring. (8) The position-limiting device. (9) The eccentric vibration device. (10) The eccentric wheel.

contact points of cutters and sugarcanes. Vibrations are translations, so the axial sugarcane cutting point vibration displacement is just the axial cutter vibration displacement at the contact moment. Sugarcanes move along the SFP, so the axial sugarcane cutting point vibration displacement was obtained though measuring the axial cutter vibration displacement. The axial cutter vibration amplitude and frequency are dependent on the eccentric distance of the eccentric wheel and the frequency of the variable-frequency velocity-adjusting motor. The frequency of the variable-frequency velocity-adjusting motor is controlled through a digital frequency convertor (Model: F1000-G0055T3B. The frequency adjusting range: 0.05 Hz~400 Hz).

3. Sugarcane Cutting Quality Evaluating Indexes

The number of sugarcane cracks, the crack thickness, and the crack length are all related to the sugarcane cutting quality (SCQ). It is difficult to use only one index to evaluate the SCQ in that their contributions to the SCQ are different, so the improved entropy method was used to calculate contribution weights of these three evaluation indexes and finally calculate the SCQ evaluating value, y [31] called the comprehensive cutting quality evaluating value (CCQEV), as is calculated through equation (1). The greater y is, the poorer the SCQ will be.

$$\begin{cases} x'_{ij} = \dfrac{x_{ij} - x_{j\min}}{x_{j\max} - x_{j\min}}, \\ p_{ij} = \dfrac{x'_{ij}}{\sum_{i=1}^{m} x'_{ij}}, \\ k = \dfrac{1}{\ln m}, \\ e_j = -k \sum_{i=1}^{m} p_{ij} \ln p_{ij}, \\ g_j = 1 - e_j, \\ w_j = \dfrac{g_j}{\sum_{j=1}^{3} g_j}, \\ y_i = \sum_{j=1}^{3} x'_{ij} w_j, \\ y = \dfrac{\sum_{i=1}^{m} y_i}{m}, \end{cases} \tag{1}$$

where: x'_{ij}, x_{ij} mean the membership degree and the maximum value of the No. j evaluation index in the No. i sugarcane cutting experiment, respectively. $j = 1, 2, 3$, corresponding to the number of sugarcane cracks, the crack thickness, and length. $i = 1, 2, 3 \ldots m$. In single-factor experiments, $m = 5$. In orthogonal experiments, $m = 1$. When $j = 1$, x'_{i1} and x_{i1} mean the membership degree and the number of sugarcane cracks in the No. i sugarcane cutting experiment, respectively. When $j = 2$, x'_{i2} and x_{i2} mean the membership degree and the maximum value of crack thicknesses in the No. i sugarcane cutting experiment, respectively. When $j = 3$, x'_{i3} and x_{i3} mean the membership degree and the maximum value of crack lengths in the No. i sugarcane cutting experiment, respectively. $x_{j_{\max}}$, $x_{j_{\min}}$ mean the maximum and the minimum values of the No. j evaluation index in all sugarcane cutting experiments, respectively. p_{ij} means the proportion of the No. j evaluation index in the No. i sugarcane cutting experiment. e_j, g_j, w_j mean the entropy value, the difference coefficient, and the contribution weight of the No. j evaluation index, respectively. $R^2 = 0.9876$ means the CCQEV of the No. i sugarcane cutting experiment. $y = 0.0376x_2 + 0.3047$ is the average value of all CCQEVs of F_p times of sugarcane cutting experiments.

4. Materials and Methods

In all experiments, fresh and straight No. 42 Guitang sugarcanes with leaves and burrs were wiped off, an average diameter of 28 ± 3 mm was adopted, and roots of 1000 mm length and upward were chosen.

The axial cutter vibration displacement was measured through a laser displacement sensor (Producer: Keyence. Model: LK-G150 A. The displacement measuring range: −40 mm–40 mm. The measuring accuracy: 0.005 mm). Three-directional cutting forces were measured through a common milling force-measuring system developed by School of Mechanical Engineering, Dalian University of Technology, with a force measuring range of −5000 N–5000 N and a measuring accuracy of 0.1 N. Block diagrams of the axial cutter vibration amplitude-measuring system and the common milling force-measuring system are shown in Figures 2 and 3.

The piezoelectric three-directional force-measuring device is shown in Figure 4. It was installed under the sugarcane-clamping device.

A laser velocity meter (Model: AR926. The rotation velocity measuring range: 0–3000 RPM) was used to measure the cutter rotation velocity. The cutter installing angle was measured through a digital inclinometer with an accuracy of 0.05° and an angle measurement range of 90°. Sugarcane crack thicknesses and lengths were measured through a vernier caliper with an accuracy of 0.02 mm to calculate the CCQEV.

An HSE1024 high-speed camera of the American NAC company was used to observe the sugarcane cutting process. Its greatest shoot frame number is 4000/s, its screen resolution is 1024×768, and its shoot rate is 1000 frames/s.

In this paper, the orthogonal experiment, single-factor experiments, and the quadratic regressive orthogonal rotational experiment were done on the SHEP.

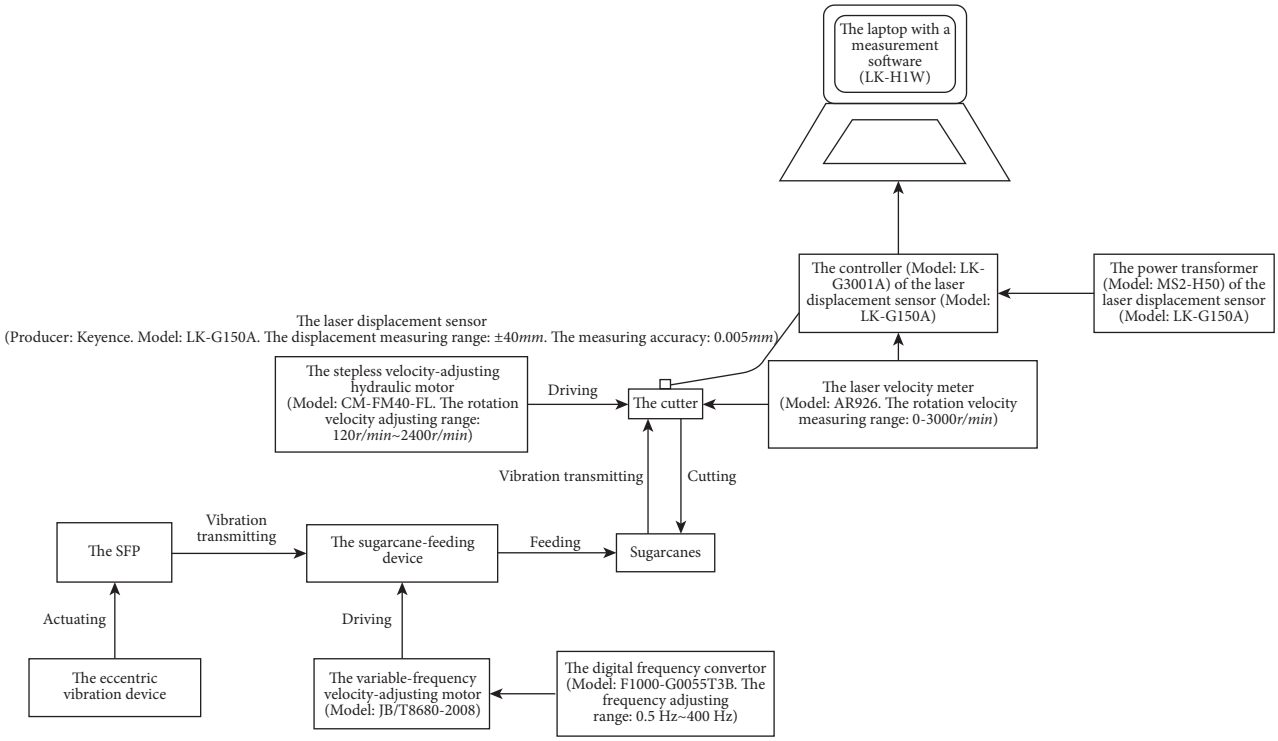

Figure 2: The block diagram of the axial cutter vibration amplitude-measuring system.

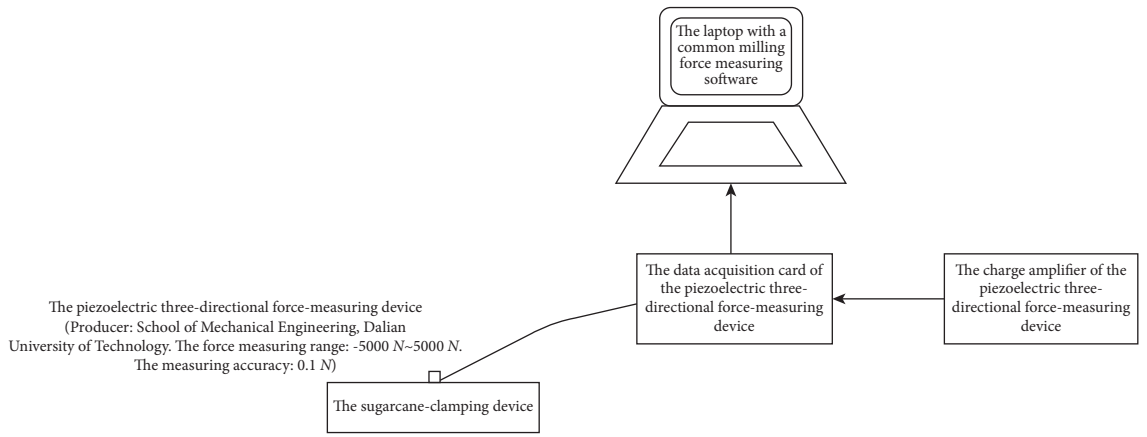

Figure 3: The block diagram of the common milling force-measuring system.

5. Design on the Orthogonal Experiment

The orthogonal experiment was aimed at studying significance levels of the effects of the amplitude and the frequency of the axial cutter vibration, the sugarcane feeding velocity, the cutter installing angle, and the cutter rotation velocity on the SCQ. Levels of these five experimental factors are shown in Table 1. Design and the result of the orthogonal experiment are shown in Tables 2 [32] and 3.

6. Design on Single-Factor Experiments

Single-factor experiments were aimed at studying the effects of the amplitude and the frequency of the axial cutter vibration on the SCQ. Levels of these two experimental factors are shown in Table 4.

Constant levels of the amplitude and the frequency of the axial cutter vibration in single-factor experiments were 4 mm and 6 Hz, respectively. Other experiment conditions were that

(a) (b) (c)

Figure 4: The piezoelectric three-directional force-measuring device (a). Three channels corresponding to the x, the y, and the z axes (b). The piezoelectric three-directional force-measuring device installed under the sugarcane-clamping device (c).

Table 1: Levels of five experimental factors of the orthogonal experiment.

Level factor	1	2
The axial cutter vibration frequency, x_1 (Hz)	9	6
The axial cutter vibration amplitude, x_2 (mm)	6.5	3.5
The cutter rotation velocity, x_3 (RPM)	700	600
The sugarcane feeding velocity, x_4 (m/s)	0.6	0.4
The cutter installing angle, x_5 (^{o})	10	0

Table 2: Design on the orthogonal experiment.

No.	Factor				
	x_1	x_2	x_3	x_4	x_5
1	1	1	1	1	1
2	1	1	1	2	2
3	1	1	2	1	2
4	1	1	2	2	1
5	1	2	1	1	2
6	1	2	1	2	1
7	1	2	2	1	1
8	1	2	2	2	2
9	2	1	1	1	2
10	2	1	1	2	1
11	2	1	2	1	1
12	2	1	2	2	2
13	2	2	1	1	1
14	2	2	1	2	2
15	2	2	2	1	2
16	2	2	2	2	1

Table 3: The orthogonal experiment result.

No.	Factor					
	x_1	x_2	x_3	x_4	x_5	The CCQEV
1	1	1	1	1	1	1
2	1	1	1	2	2	0.7118
3	1	1	2	1	2	0.6981
4	1	1	2	2	1	0.5191
5	1	2	1	1	2	0.0518
6	1	2	1	2	1	0.25

Table 3: Continued.

No.	Factor					
	x_1	x_2	x_3	x_4	x_5	The CCQEV
7	1	2	2	1	1	0.4618
8	1	2	2	2	2	0.1037
9	2	1	1	1	2	0.4672
10	2	1	1	2	1	0.34
11	2	1	2	1	1	0.5382
12	2	1	2	2	2	0.2691
13	2	2	1	1	1	0.1418
14	2	2	1	2	2	0
15	2	2	2	1	2	0.3909
16	2	2	2	2	1	0.2309

Table 4: Levels of two experimental factors of single-factor experiments.

Level factor	1	2	3	4	5
The axial cutter vibration amplitude (mm)	2	3.5	5	6.5	10
The axial cutter vibration frequency (Hz)	6	7	8	9	10

the sugarcane feeding velocity was 0.4 *m/s*, the cutter installing angle was 0°, and the cutter rotation velocity was 600 RPM. Every group of single-factor experiments were done five times. Single-factor experiment results are shown in Tables 5 and 6.

7. Design on the Quadratic Regressive Orthogonal Rotational Experiment

The quadratic regressive orthogonal rotational experiment was aimed at obtaining the mathematical relationship equation on the amplitude and the frequency of the axial cutter vibration, the sugarcane feeding velocity, the cutter installing angle, and the cutter rotation velocity. Levels of these five experimental factors (5 factors and 1/2 operation) are shown in Table 7 [32]. Design and the result of the quadratic regressive orthogonal rotational experiment are shown in Tables 8 [32] and 9.

8. Experiment Results and Analysis

8.1. Experiment Results. All experiment results are shown in Tables 3, 5, 6, and 9.

8.2. Analysis on the Orthogonal Experiment Result. According to Table 3, the variance analysis result of the orthogonal experiment obtained through SPSS is shown in Table 10.

According to Table 10, the following are obtained.

(1) P values of the amplitude and the frequency of the axial cutter vibration are smaller than 0.05, so their effects on the CCQEV are significant, and so they were used to do single-factor experiments to further study their effects on the CCQEV.

(2) P values of the cutter rotation velocity, the sugarcane feeding velocity, and the cutter installing angle are greater than 0.05, so their effects on the CCQEV are not significant, so they were not used to do single-factor experiments.

(3) According to F values, significance levels of effects of these five experimental factors from high to low are as follows, the axial cutter vibration amplitude, the axial cutter vibration frequency, the sugarcane feeding velocity, the cutter rotation velocity, and the cutter installing angle.

8.3. Analysis on Single-Factor Experiment Results

8.3.1. Analysis on the Effect of the Axial Cutter Vibration Amplitude on the CCQEV. According to Table 5, the fitting curve of the CCQEV changing with the axial cutter vibration amplitude drawn through Excel is shown in Figure 5.

According to Figure 5, the greater the axial cutter vibration amplitude is, the greater the CCQEV will be, that is, the poorer the SCQ will be.

According to Figure 5, the fitting equation of the fitting curve of the CCQEV changing with the axial cutter vibration amplitude is shown in equation (2). The determination coefficient of equation (2) is $R^2 = 0.9876$, so this fitting curve and its fitting equation have high fitting degrees.

$$y = 0.0376x_2 + 0.3047. \quad (2)$$

According to Table 5, the correlation analysis result of the axial cutter vibration amplitude and the CCQEV obtained through SPSS is shown in Table 11.

According to Table 11, the significance coefficient between the axial cutter vibration amplitude and the CCQEV is 0, so there is a strong correlation relationship between the axial cutter vibration amplitude and the CCQEV. Moreover, the correlation coefficient between the axial cutter vibration amplitude and the CCQEV is $0.997 > 0$, so there is a strong positive correlation relationship between the axial cutter vibration amplitude and the CCQEV, verifying the discovery obtained through Figure 5.

8.3.2. Analysis on the Effect of the Axial Cutter Vibration Frequency on the CCQEV. According to Table 6, the fitting curve of the CCQEV changing with the axial cutter vibration frequency drawn through Excel is shown in Figure 6.

According to Figure 6, the greater the axial cutter vibration frequency is, the greater the CCQEV will be, that is, the poorer the SCQ will be.

Table 5: The single-factor experiment result with the axial cutter vibration amplitude as the single factor.

No. of the axial cutter vibration amplitude (mm)	1	2	3	4	5	The average value of CCQEVs obtained in the five repetitive experiments	The standard deviation of CCQEVs obtained in the five repetitive experiments
2	0.36	0.37	0.38	0.365	0.375	0.37	0.007906
3.5	0.43	0.44	0.45	0.435	0.445	0.44	0.0095
5	0.48	0.49	0.5	0.485	0.495	0.49	0.008754
6.5	0.56	0.57	0.58	0.565	0.575	0.57	0.007852
10	0.66	0.67	0.68	0.665	0.675	0.67	0.007004

Table 6: The single-factor experiment result with the axial cutter vibration frequency as the single factor.

No. of the axial cutter vibration frequency (Hz)	1	2	3	4	5	The average value of CCQEVs obtained in the five repetitive experiments	The standard deviation of CCQEVs obtained in the five repetitive experiments
6	0.32	0.33	0.34	0.325	0.335	0.33	0.007906
7	0.41	0.42	0.43	0.415	0.425	0.42	0.009618
8	0.44	0.45	0.46	0.445	0.455	0.45	0.008732
9	0.53	0.54	0.55	0.535	0.545	0.54	0.006981
10	0.6	0.61	0.62	0.605	0.615	0.61	0.007391

Table 7: Levels of five experimental factors of the quadratic regressive orthogonal rotational experiment.

Factor level	x_1	x_2	x_3	x_4	x_5
The upper asterisk arm (+2.0) γ	10	8	750	0.7	15
The upper level (+1)	9	6.5	700	0.6	10
The zero level (0)	8	5	650	0.5	5
The lower level (−1)	7	3.5	600	0.4	0
The lower asterisk arm (−2.0) $-\gamma$	6	2	550	0.3	−5
Δ_j	1	1.5	50	0.1	5

Table 8: Design on the quadratic regressive orthogonal rotational experiment.

No.	Factor				
	x_1	x_2	x_3	x_4	x_5
1	1	1	1	1	1
2	1	1	1	−1	−1
3	1	1	−1	1	−1
4	1	1	−1	−1	1
5	1	−1	1	1	−1
6	1	−1	1	−1	1
7	1	−1	−1	1	1
8	1	−1	−1	−1	−1
9	−1	1	1	1	−1
10	−1	1	1	−1	1
11	−1	1	−1	1	1
12	−1	1	−1	−1	−1
13	−1	−1	1	1	1
14	−1	−1	1	−1	−1
15	−1	−1	−1	1	−1
16	−1	−1	−1	−1	1
17	2	0	0	0	0
18	−2.0	0	0	0	0
19	0	2.0	0	0	0
20	0	−2.0	0	0	0
21	0	0	2.0	0	0
22	0	0	−2.0	0	0

Table 8: Continued.

No.	Factor				
	x_1	x_2	x_3	x_4	x_5
23	0	0	0	2.0	0
24	0	0	0	−2.0	0
25	0	0	0	0	2.0
26	0	0	0	0	−2.0
27	0	0	0	0	0
28	0	0	0	0	0
29	0	0	0	0	0
30	0	0	0	0	0
31	0	0	0	0	0
32	0	0	0	0	0
33	0	0	0	0	0
34	0	0	0	0	0
35	0	0	0	0	0
36	0	0	0	0	0

Table 9: The quadratic regressive orthogonal rotational experiment result.

No.	Factor					
	x_1	x_2	x_3	x_4	x_5	The CCQEV
1	1	1	1	1	1	1
2	1	1	1	−1	−1	0.7118
3	1	1	−1	1	−1	0.6981
4	1	1	−1	−1	1	0.5191
5	1	−1	1	1	−1	0.0518
6	1	−1	1	−1	1	0.25
7	1	−1	−1	1	1	0.4618
8	1	−1	−1	−1	−1	0.1037
9	−1	1	1	1	−1	0.4672
10	−1	1	1	−1	1	0.34
11	−1	1	−1	1	1	0.5382
12	−1	1	−1	−1	−1	0.2691
13	−1	−1	1	1	1	0.1418
14	−1	−1	1	−1	−1	0
15	−1	−1	−1	1	−1	0.3909
16	−1	−1	−1	−1	1	0.2309
17	2	0	0	0	0	0.9291
18	−2.0	0	0	0	0	0.4154
19	0	2.0	0	0	0	0.7881
20	0	−2.0	0	0	0	0.3009
21	0	0	2.0	0	0	0.5181
22	0	0	−2.0	0	0	0.3254
23	0	0	0	2.0	0	0.5563
24	0	0	0	−2.0	0	0.3009
25	0	0	0	0	2.0	0.3963
26	0	0	0	0	−2.0	0.2636
27	0	0	0	0	0	0.589
28	0	0	0	0	0	0.3527
29	0	0	0	0	0	0.4472
30	0	0	0	0	0	0.4809
31	0	0	0	0	0	0.4692
32	0	0	0	0	0	0.6272
33	0	0	0	0	0	0.779
34	0	0	0	0	0	0.4472
35	0	0	0	0	0	0.3664
36	0	0	0	0	0	0.5754

Table 10: The variance analysis result of the orthogonal experiment.

Source	Sum of squares	Freedom degree	Variance	F	P
Corrected model	0.914	6	0.152	6.353	0.007
Intercept	2.361	1	2.361	98.451	0.000
The axial cutter vibration frequency	0.129	1	0.129	5.395	0.045
The axial cutter vibration amplitude	0.531	1	0.531	22.151	0.001
The cutter rotation velocity	0.034	1	0.034	1.414	0.265
The sugarcane feeding velocity	0.114	1	0.114	4.774	0.057
The cutter installing angle	0.005	1	0.005	0.224	0.647
Error	0.216	9	0.024		
Total	3.491	16			
Corrected total	1.130	15			

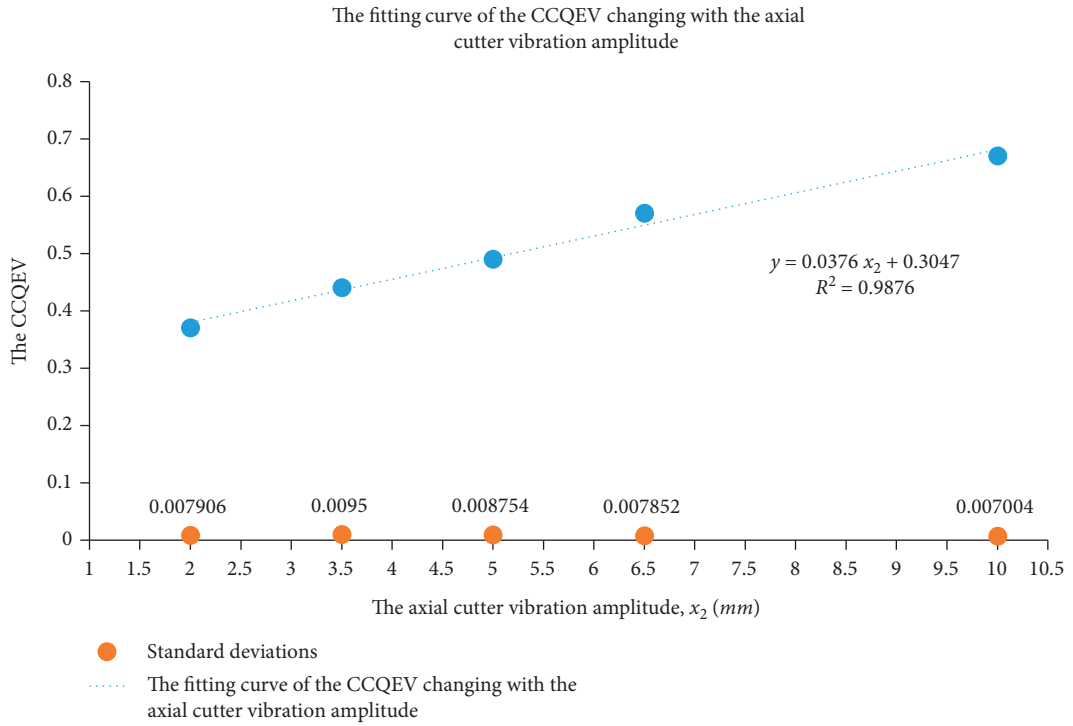

Figure 5: The fitting curve of the CCQEV changing with the axial cutter vibration amplitude.

Table 11: The correlation analysis result of the axial cutter vibration amplitude and the CCQEV.

	Correlation coefficient	Significance coefficient
The axial cutter vibration amplitude-the CCQEV	0.997	0.000

According to Figure 6, the fitting equation of the curve of the CCQEV changing with the axial cutter vibration frequency is shown in equation (3). The determination coefficient of equation (3) is $R^2 = 0.9838$, so this fitting curve and its fitting equation have high fitting degrees.

$$y = 0.068x_1 + 0.074. \quad (3)$$

According to Table 6, the correlation analysis result of the axial cutter vibration frequency and the CCQEV obtained through SPSS is shown in Table 12.

According to Table 12, the significance coefficient between the axial cutter vibration frequency and the CCQEV is 0.028, so there is a strong correlation relationship between the axial cutter vibration frequency and the CCQEV. Moreover, the correlation coefficient between the axial cutter vibration frequency and the CCQEV is $0.918 > 0$, so there is a strong positive correlation relationship between the axial cutter vibration frequency and the CCQEV, verifying the discovery obtained through Figure 6.

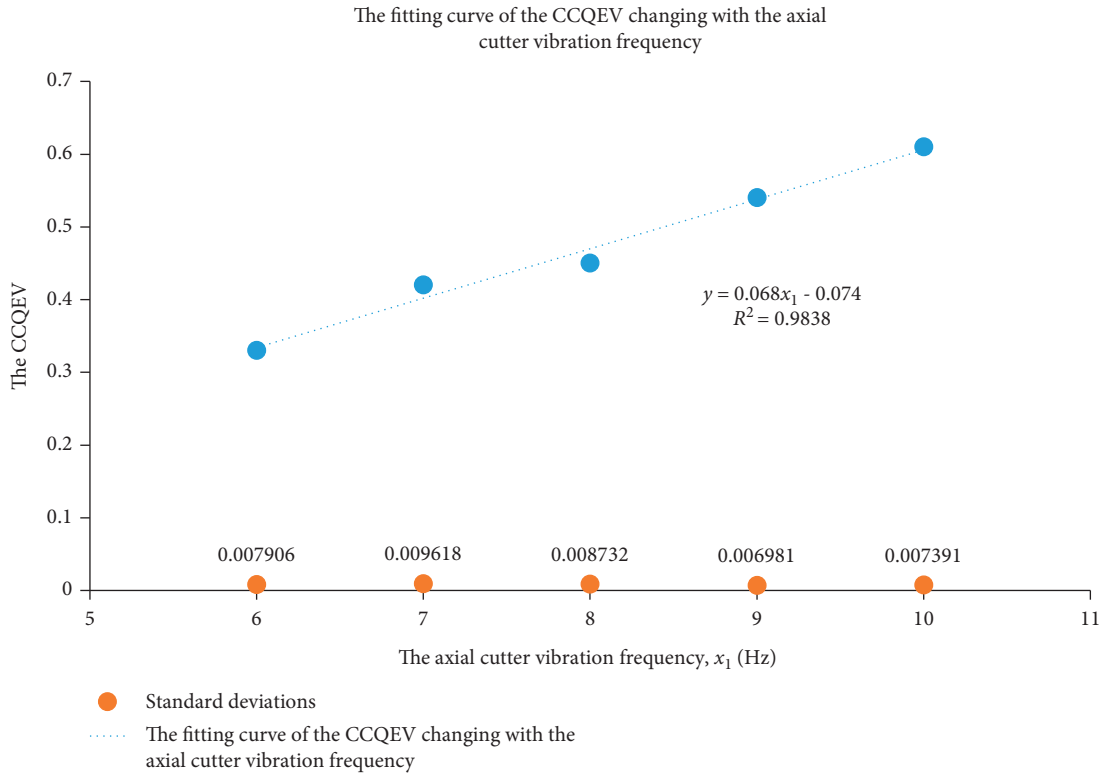

Figure 6: The fitting curve of the CCQEV changing with the axial cutter vibration frequency.

Table 12: The correlation analysis result of the axial cutter vibration frequency and the CCQEV.

	Correlation coefficient	Significance coefficient
The axial cutter vibration frequency—the CCQEV	0.918	0.028

8.4. Analysis on the Quadratic Regressive Orthogonal Rotational Experiment Result

8.4.1. The Regressive Equation. According to Table 9, the regressive equation of five experimental factors and the CCQEV obtained through SPSS is shown in

$$\hat{y} = 0.388 - 0.007x_1 - 0.868x_2 + 0.0098x_3 + 0.294x_4 + 0.024x_5 + 0.051x_1x_2 + 0.001x_2x_3 - 0.0000148x_3^2 - 0.14x_4^2 - 0.0024x_5^2. \quad (4)$$

P values of the regressive equation are shown in Table 13.

According to Table 13, P values of most coefficients and equation (4) are smaller than 0.05 except P values of coefficients of x_5, x_3^2, and x_4^2, so equation (4) and its coefficients have high accuracy.

8.4.2. Analysis on the Effects of Other Experimental Factors on the CCQEV. Equation (4) was used to analyze effects of other experimental factors on the CCQEV. According to equation (4), with other symbols being 0, respectively, except the cutter rotation velocity, the sugarcane feeding velocity, and the cutter installing angle, curves of the CCQEV changing with the cutter rotation velocity, the sugarcane feeding velocity, and the cutter installing angle drawn through MATLAB are shown in Figures 7(a) to 7(c).

These three curves are value simulating calculation results of relationships between the CCQEV and the cutter rotation velocity, the CCQEV and the sugarcane feeding velocity, the CCQEV and the cutter installing angle. According to Figure 7(a), the greater the cutter rotation velocity is, the smaller the CCQEV will be, that is, the better the SCQ will be. According to Figure 7(b), the greater the sugarcane feeding velocity is, the greater the CCQEV will be, that is, the poorer the SCQ will be. According to Figure 7(c), with the cutter installing angle increasing, the CCQEV became greater firstly. It reached the maximum value when the cutter installing angle was 5°, that is, the SCQ is the poorest. Then, the CCQEV became smaller.

8.4.3. Analysis on Interaction Effects on the CCQEV. According to (4), with other symbols being 0, respectively, except the amplitude and the frequency of the axial cutter vibration, the axial cutter vibration amplitude, and the cutter rotation velocity, surface diagrams of the CCQEV changing with interaction between the amplitude and the frequency of the axial cutter vibration and interaction

Table 13: P values of equation (4) and its coefficients.

Item	b_0	b_1	b_2	b_3	b_4	b_5	b_{12}	b_{23}	b_{33}	b_{44}	b_{55}	Equation	Standard deviation
P	0	0	0	0	0.004	0.077	0.016	0.014	0.085	0.099	0.007	0.001	0.13

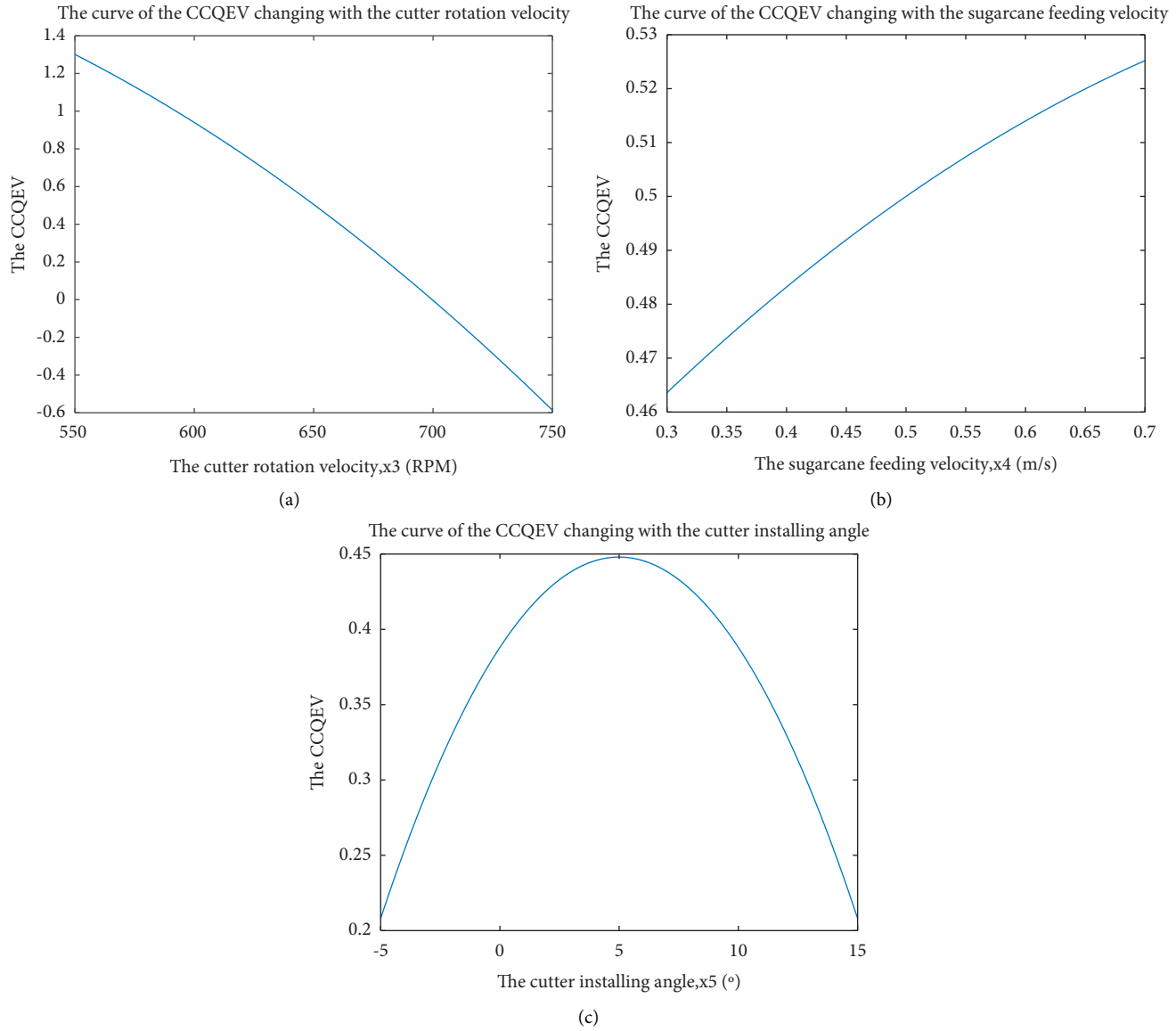

Figure 7: Curves of the CCQEV changing with (a) the cutter rotation velocity, (b) the sugarcane feeding velocity, and (c) the cutter installing angle.

between the axial cutter vibration amplitude and the cutter rotation velocity drawn through MATLAB are shown in Figures 8 and 9.

Figure 8 is the value simulating calculation result of the relationship between the CCQEV and interaction between the amplitude and the frequency of the axial cutter vibration. According to Figure 8, the greater the amplitude and the frequency of the axial cutter vibration are, the greater the CCQEV will be, that is, the poorer the SCQ will be. Under a constant axial cutter vibration frequency, the greater the axial cutter vibration amplitude is, the greater the CCQEV will be, that is, the poorer the SCQ will be. Under constant axial cutter vibration amplitude, the greater the axial cutter vibration frequency is, the greater the CCQEV will be, that is, the poorer the SCQ will be.

Figure 9 is the value simulating calculation result of the relationship between the CCQEV and interaction between the axial cutter vibration amplitude and the cutter rotation velocity. According to Figure 9, the greater the axial cutter vibration amplitude and the cutter rotation velocity are, the greater the CCQEV will be, that is, the poorer the SCQ will

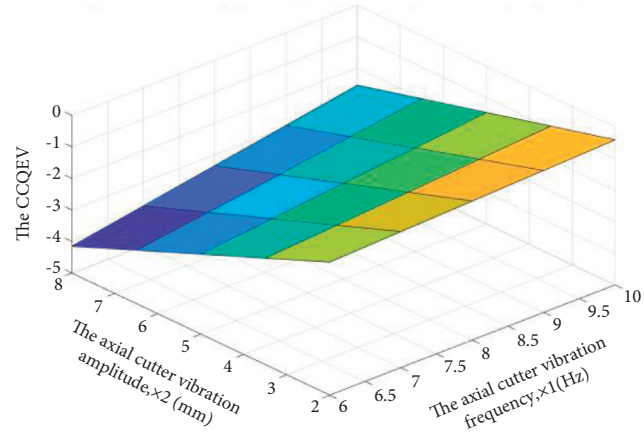

Figure 8: The surface diagram of the CCQEV changing with the interaction between the amplitude and the frequency of the axial cutter vibration.

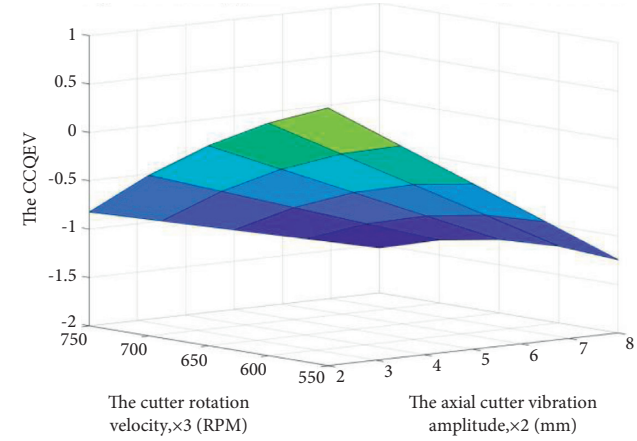

Figure 9: The surface diagram of the CCQEV changing with the interaction between the axial cutter vibration amplitude and the cutter rotation velocity.

be in that according to analysis on the orthogonal experiment result, the effect of the axial cutter vibration amplitude on the CCQEV is the most significant while the effect of the cutter rotation velocity is not significant, so the major effect is caused by the axial cutter vibration amplitude, making the CCQEV greater, that is, the SCQ poorer. Under a constant cutter rotation velocity, the greater the axial cutter vibration amplitude is, the greater the CCQEV will be, that is, the poorer the SCQ will be. Under a constant axial cutter vibration amplitude, the greater the cutter rotation velocity is, the smaller the CCQEV will be, that is, the better the SCQ will be.

In conclusion, according to Figures 5–7, for small sugarcane harvesters in hilly areas, the smaller the amplitude and the frequency of the axial cutter vibration are, the better the SCQ will be, and best values of the cutter rotation velocity, the sugarcane feeding velocity, and the cutter installing angle are 750 RPM, 0.7 m/s, and 15°.

9. Analysis on the Sugarcane Cutting Mechanism

9.1. Analysis on Cutting Force Signals. Cutting force signals obtained through the common milling force-measuring system were saved as Excel files and imported into MATLAB. The wavelet analysis tool of MATLAB was used to do noise reduction to study how sugarcane is cut off by cutters. When cutting forces were measured, as is mentioned above, the axial cutter vibration amplitude was set as 4 mm, the axial cutter vibration frequency was set as 2 Hz, the cutter rotation velocity was set as 750*RPM*, the sugarcane feeding velocity was set as 0.7 *m/s*, and the cutter installing angle was set as 15°. Original cutting force signals are shown in Figure 10.

According to Figure 10, there existed a lot of environmental noises. Wave crests in Figure 10 mean shocks suffered by the sugarcane.

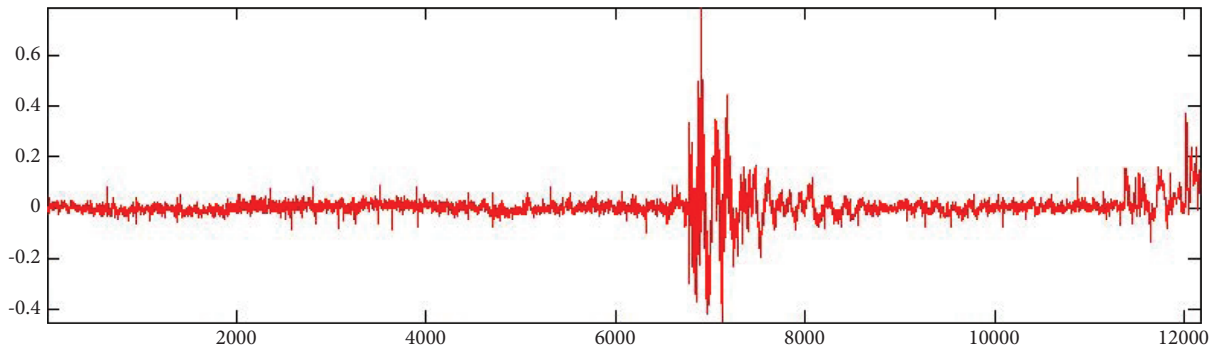

Figure 10: Original cutting force signals.

Wavelet analysis results of these original cutting force signals obtained through the db5 wavelet packet are shown in Figure 11.

In Figure 11, Figure 10 is denoted as s and it was decomposed into $a5$, $d1$, $d2$, $d3$, $d4$, and $d5$. $a5$ is the signal obtained after five times of noise reduction decompositions of Figure 10, and it is shown clearly in Figure 12. $d1$, $d2$, $d3$, $d4$, and $d5$ are high-frequency parts of Figure 10.

According to Figure 12, the front part of cutting force signals is smooth and steady with small fluctuations, showing that the environment had an actuating effect on the force-measuring device. There existed deformations and irregularities in the SFP, so vibrations were caused when the sugarcane-feeding device traveled along the SFP, generating fluctuations. Then, three high wave crests appear in Figure 12 and intervals between every two wave crests are the same, showing the cutters crushed the sugarcane and the sugarcane was cut off in three times of cutting. In the wake of these three wave crests, Figure 12 becomes smooth and steady again, showing that the sugarcane-feeding device went on to travel for some distances along the SFP. Besides, the resonance phenomenon of the SHEP during the sugarcane cutting process also caused fluctuations in the front part of Figure 12.

9.2. Analysis on the High-Speed Photographing Result in the Sugarcane Cutting Process. High-speed photographing was aimed at studying interaction between blades and sugarcanes and verifying the discovery obtained through analysis on cutting force signals. Some video screenshots are shown in Figures 13–16.

According to Figures 13–16, a sugarcane was cut off by several times of cutting. The least number of cutting times was two and the greatest number was four, matching analysis on cutting force signals. There was an obvious height difference between two cut-in points because of relative axial displacements between blades and sugarcanes caused by the axial cutter vibration. The second cut-in pint was higher or lower than the first one. This is dependent on positions of the blades and the first cut-in point in the second time of cutting and whether the axial cutter vibration was upward or downward. According to Figure 13, the sugarcane was cut off in two times of cutting and the second cut-in point was higher than the first one. According to Figure 14, the sugarcane was also cut off in two times of cutting and the second cut-in point was lower than the first one. According to Figure 15, the sugarcane was cut off in three times of cutting and the first cut-in point was lower than the second one. According to Figure 16, there was an obvious height difference between two clear cuts left during two times of cutting. The second cut-in point was higher than the first one.

The sugarcane root after being cut off is shown in Figure 17.

According to Figure 17, there are obvious stairs and axial cracks caused by the axial cutter vibration and the axial cutter vibration also led to relative axial displacements between blades and the sugarcane.

9.3. Simulations of the Sugarcane Cutting Process under Vibration Excitations. Simulations of the sugarcane cutting process under vibration excitations were aimed at further studying the sugarcane cutting mechanism. According to analysis on cutting force signals and the high-speed photographing result in the sugarcane cutting process, a sugarcane was cut off by several times of cutting, so simulations were separated into two situations that a sugarcane was cut for the first time and for the second time.

9.3.1. Simulation of the Sugarcane Cutting Process without Lateral Sugarcane Cracks under Dynamic Loads (That Is, a Sugarcane Is Cut for the First Time). In this simulation, the sugarcane diameter was set as 30 mm. The sugarcane length was set as 250 mm in that cutters only have effects in small areas of sugarcane roots. The cutter model was established as a blade with an 80 mm length and a 5 mm thickness according to sizes of the cutters of the SHEP. Models of the cutter and the sugarcane established in UG8.0 were imported into Hypermesh14.0. Meshes were generated in these two models. The No. 20 rigid body material was chosen as the material of the cutter and the No. 22 composite material was chosen as the material of the sugarcane with its elasticity moduli along and vertical to the fiber direction being 813 MPa and 152.5 MPa, its Poisson ratios being $\mu_{xy} = 0.53$, $\mu_{yx} = 0.105$, $\mu_{yz} = 0.265$, and its shear moduli along its isotropic surface and anisotropic surface being 17.75 MPa and 1.14 MPa. The solid64 unit was chosen as meshes of these

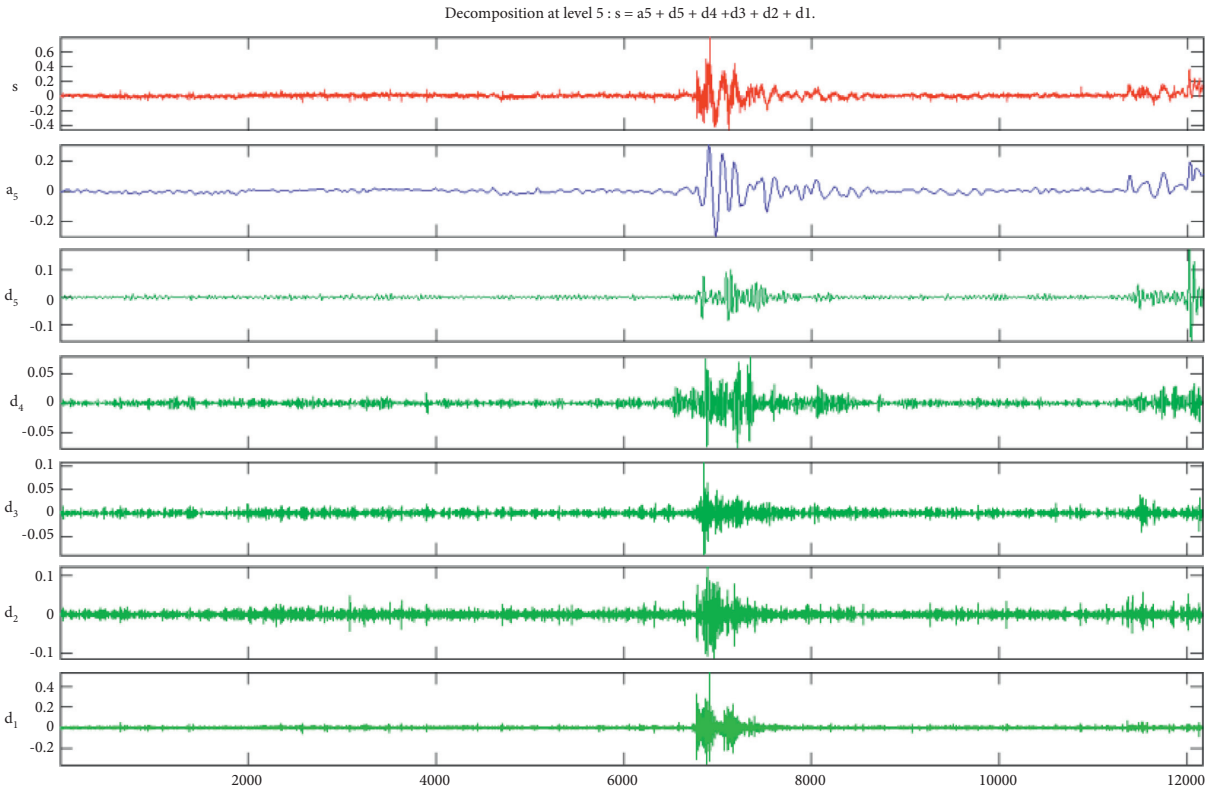

Figure 11: Wavelet analysis results of original cutting force signals.

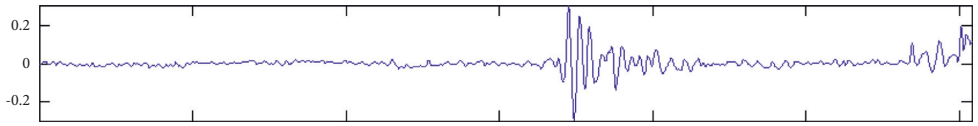

Figure 12: The signal obtained after noise reduction processing of original cutting forces.

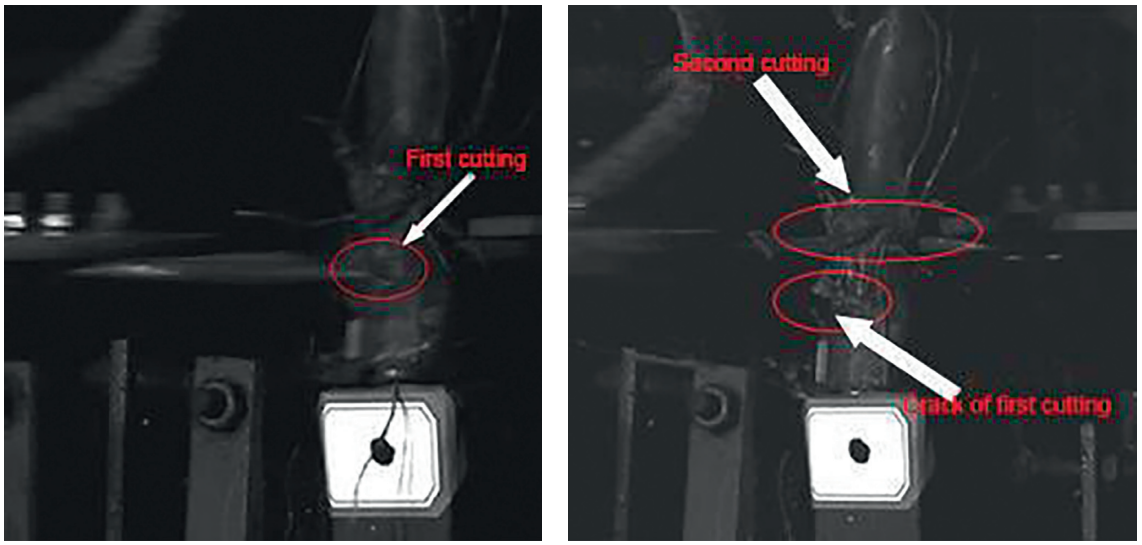

(a) (b)

Figure 13: The second cut-in point was higher than the first one. (a) The first cut-in point. (b) The second cut-in point.

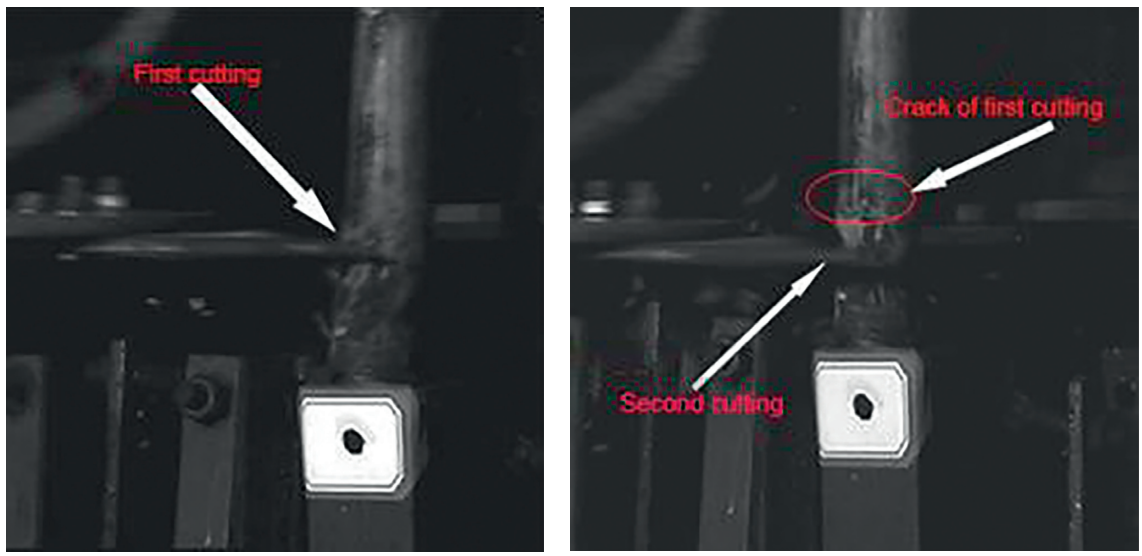

(a) (b)

Figure 14: The second cut-in point was lower than the first one. (a) The first cut-in point. (b) The second cut-in point.

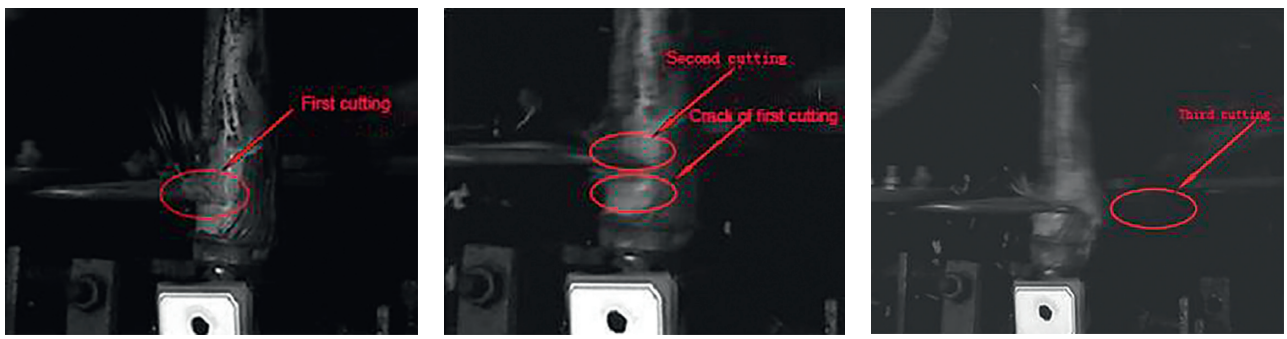

(a) (b) (c)

Figure 15: Three cut-in points. (a) The first cut-in point. (b) The second cut-in point. (c) The third cut-in point.

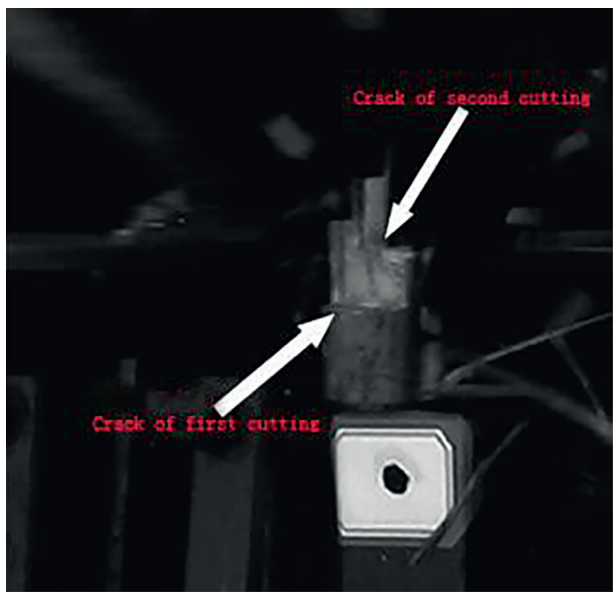

Figure 16: The height difference between two cut-in points.

Figure 17: The sugarcane with stairs after being cut off.

two models. The total mesh number was 99708 in which the mesh number of the cutter model was 5325 and the mesh number of the sugarcane model was 87048. Mesh densities were different in different areas of the sugarcane model. Meshes were refined and the mesh density was increased on contact surfaces of the sugarcane and the cutter to ensure that the solution accuracy could be improved when the solution and operation amount was increased. The size of these meshes was 0.1 mm. Meshes of other parts of the sugarcane model were relatively sparse with the size of 1 mm. As is mentioned above, the cutter rotation velocity was set as 750 RPM.

The cutter and the sugarcane models after mesh generation are shown in Figure 18. Facet erosion contact was established in models of the cutter and the sugarcane. There were no freedom degrees in lower areas of the sugarcane model. The y axis is along the axis of the sugarcane, that is, the fiber direction and the x axis is along the cut-in direction.

This simulation was designed as a single-factor experiment and the experimental factor is the axial cutter vibration amplitude with four levels, 2 mm, 4 mm, 6 mm, and 8 mm, to study effects of the axial cutter vibration amplitude on the resultant cutting force, the axial cutting force along the y axis, and the absolute value of the radial cutting force along the x axis.

After preprocessing of the simulation model done in Hyper14.0, the exported K file was imported into the LS-DYNA971 solver. LSPREPOST was used to check the post-processing result. Curves of the resultant cutting force, the axial cutting force along the y axis denoted as F_p, and the absolute value of the radial cutting force along the x axis denoted as F_f changing with time are shown in Figure 19.

Maximum values of the resultant cutting force, F_f and F_p are shown in Table 14.

According to Figure 19, the maximum value of the resultant cutting force appeared at the point of 0.75 mm where the cutter cut into the half of the sugarcane and fluctuations of the resultant cutting force appeared in the cut-in process in that the sugarcane was an elastomer and the axial cutter vibration appeared, causing a shaking phenomenon in the cut-in process, which made axial and radial contacts between the cutter and the sugarcane change with time. According to F_f and F_p in Figure 19, fluctuations also appeared in curves of these two-directional cutting forces. Two wave crests and a wave trough appeared in curves of F_p. Directions of F_f and F_p are opposite. The axial shaking phenomenon between the cutter and the sugarcane made the upper and the lower parts of the sugarcane press the cutter, respectively. This caused fluctuations in the curves of F_f and F_p.

Fitting curves of the resultant cutting force F_f and F_p changing with the axial cutter vibration amplitude are shown in Figure 20.

According to Figure 20, the greater the axial cutter vibration amplitude is, the greater the resultant cutting force, F_f and F_p will be. Fitting equations of the resultant cutting force, F_f and F_p changing with the axial cutter vibration amplitude are shown in

$$F_r = 14.05x + 288.5, \tag{5}$$

$$F_f = -12.298x - 108.5, \tag{6}$$

$$F_p = 40.111x - 127.07. \tag{7}$$

Determination coefficients of equations (5)–(7) are 0.9849, 0.9657, and 0.7456, showing these three fitting curves and their fitting equations have high fitting degrees.

According to correlation analysis results of the axial cutter vibration amplitude and these three-directional cutting forces obtained through SPSS, correlation coefficients between the axial cutter vibration amplitude and the resultant cutting force, between the axial cutter vibration amplitude and F_f, between the axial cutter vibration amplitude and F_p are 0.99, 0.98, and 0.96, and their correlation relationships are significant. Therefore, there is a strong positive correlation relationship between the axial cutter vibration amplitude and F_p in that the axial cutter vibration makes cutters press the sugarcane upwards and downwards. The greater the axial cutter vibration amplitude is, the more significant the pressing phenomenon will be, causing F_p to be greater.

According to the correlation coefficient result of F_f and F_p obtained through SPSS, their correlation coefficient is 0.9

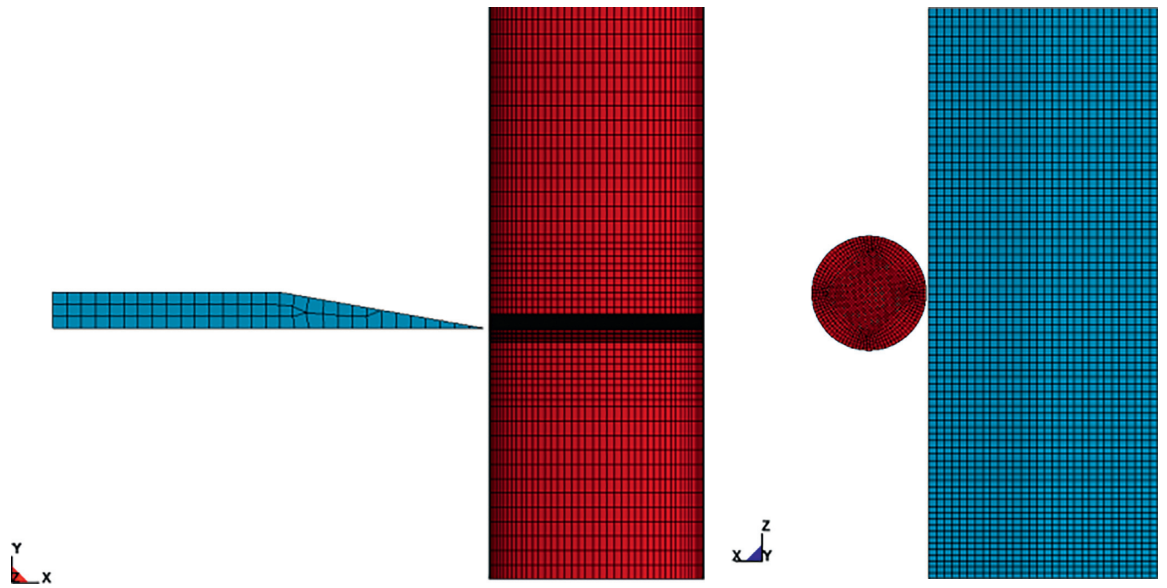

Figure 18: The simulation model without lateral sugarcane cracks under dynamic loads. (a) The front view of the simulation model. (b) The top view of the simulation model.

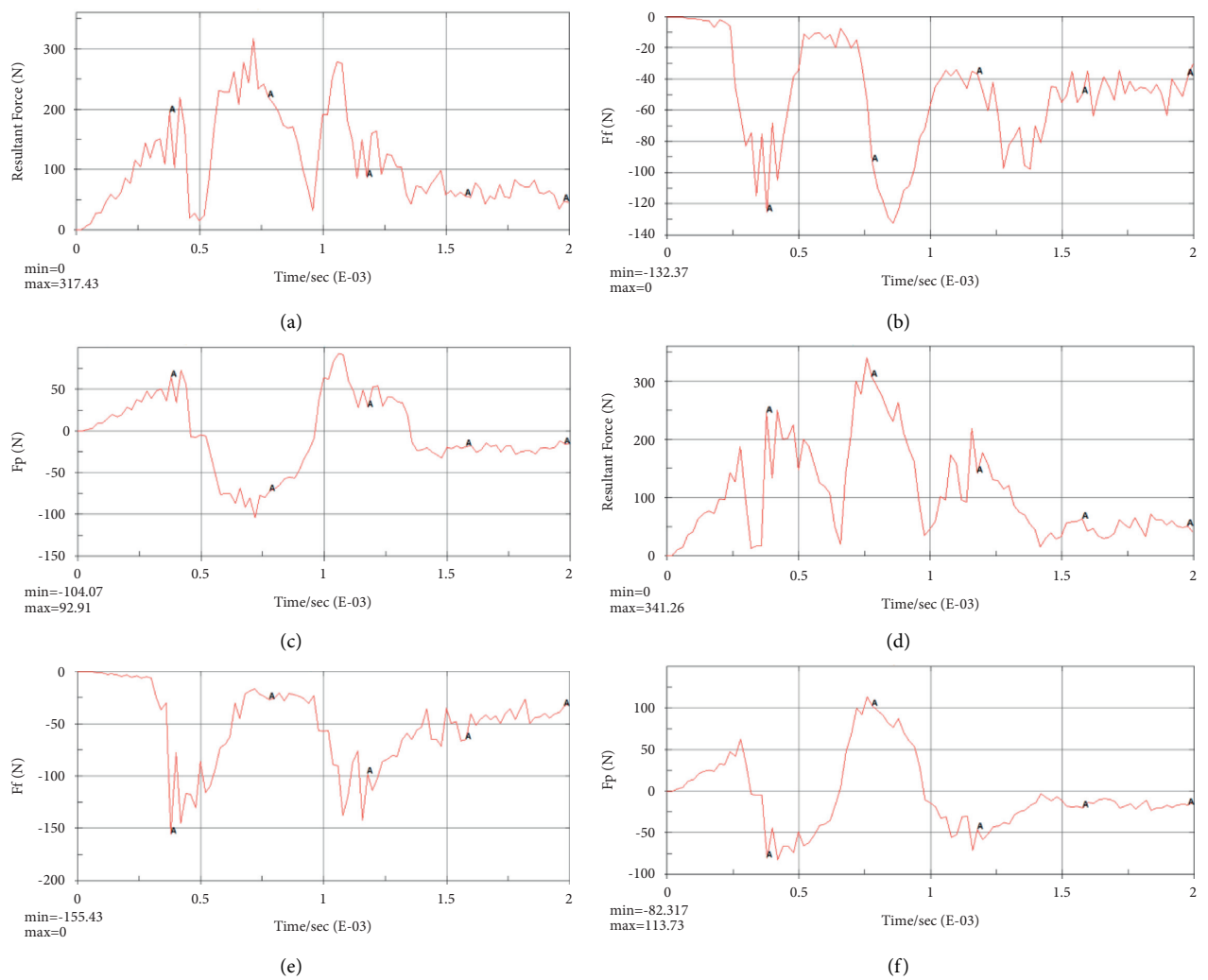

Figure 19: Continued.

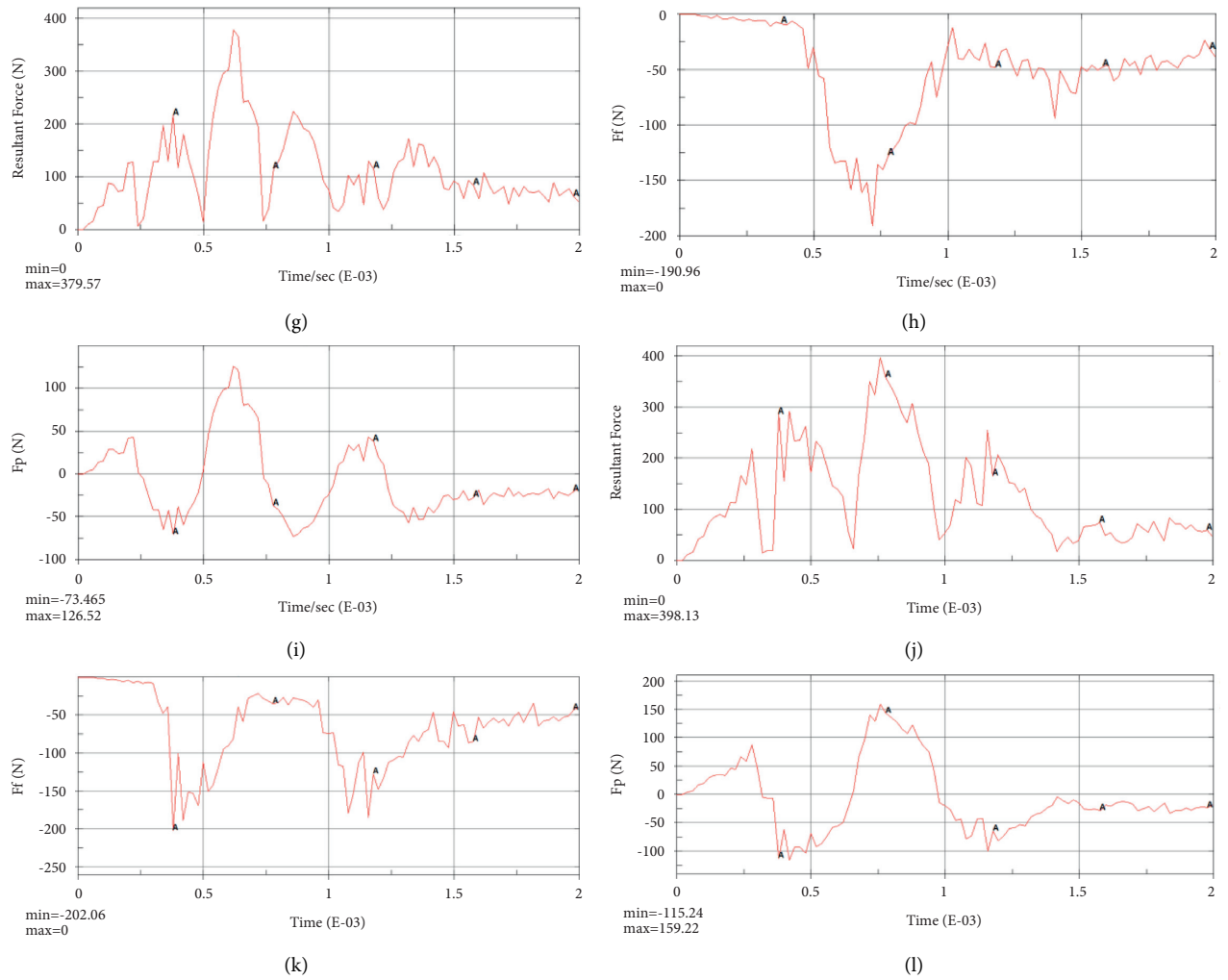

Figure 19: Curves of the resultant cutting force, F_f and F_p changing with time under different axial cutter vibration amplitudes. (a) The resultant cutting force under an axial cutter vibration amplitude of 2 mm. (b) F_f under an axial cutter vibration amplitude of 2 mm. (c) F_p under an axial cutter vibration amplitude of 2 mm. (d) The resultant cutting force under an axial cutter vibration amplitude of 4 mm. (e) F_f under an axial cutter vibration amplitude of 4 mm. (f) F_p under an axial cutter vibration amplitude of 4 mm. (g) The resultant cutting force under an axial cutter vibration amplitude of 6 mm. (h) F_f under an axial cutter vibration amplitude of 6 mm. (i) F_p under an axial cutter vibration amplitude of 6 mm. (j) The resultant cutting force under an axial cutter vibration amplitude of 8 mm. (k) F_f under an axial cutter vibration amplitude of 8 mm. (l) F_p under an axial cutter vibration amplitude of 8 mm.

Table 14: Maximum values of cutting forces under different axial cutter vibration amplitudes.

The axial cutter vibration amplitude (mm)	The resultant cutting force (N)	F_f (N)	F_p (N)
2	317	−132	−104.07
4	341	−155	113
6	379	−190.96	126
8	398	−202	159

and their correlation relationship is significant in that the greater the axial cutter vibration amplitude is, the greater the F_p will be and a friction force exists between cutters and the sugarcane. The friction force is related to pressures between cutters and the sugarcane, that is, the greater these pressures are, the greater the friction force will be and the direction of the friction force is opposite to the radial cutter motion direction. This explains why there is a strong positive correlation relationship between the axial cutter vibration amplitude and F_f.

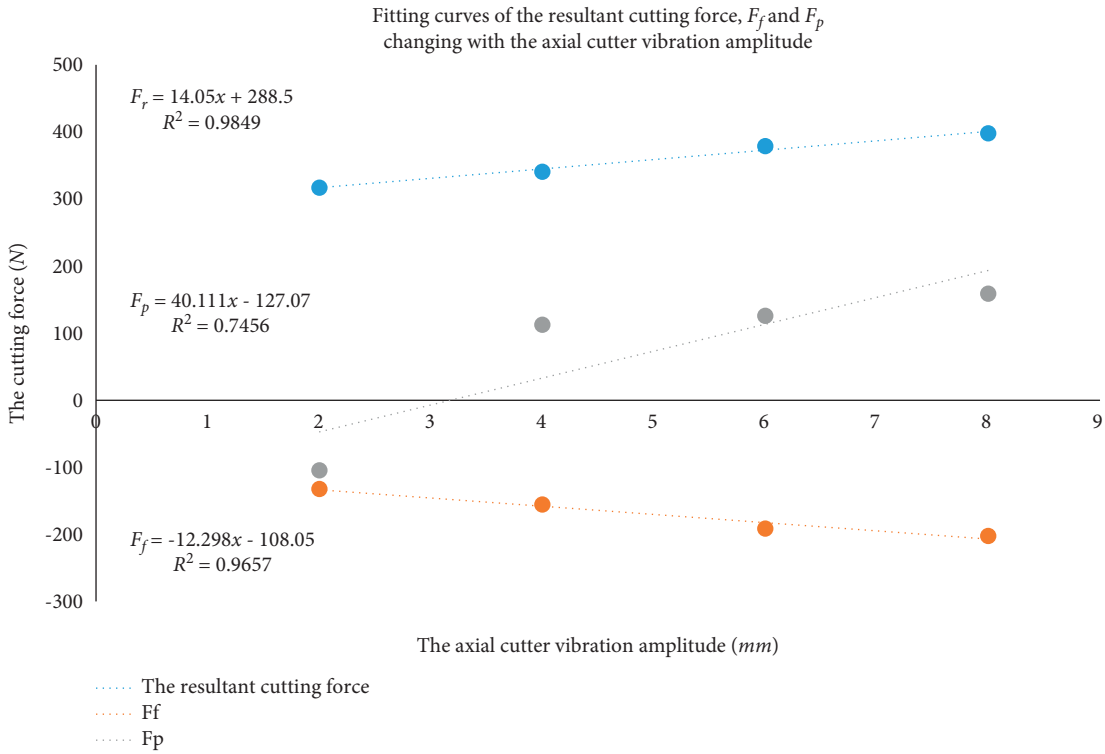

Figure 20: Fitting curves of the resultant cutting force, F_f and F_p changing with the axial cutter vibration amplitude.

9.3.2. Simulation of the Sugarcane Cutting Process with Lateral Sugarcane Cracks under Dynamic Loads (That Is, a Sugarcane Is Cut for the Second Time). Lateral sugarcane cracks will be generated after a sugarcane is cut for once. When the sugarcane is cut for the second time, the cut-in direction is random and the cut-in angle is between 0° and 90°. In this simulation, the cut-in angle was set as 90° and the sugarcane was set to be cut along the side surface of its lateral crack. The simulation model and its simulation parameters were the same as those of the previous simulation except that a lateral crack with a cut-in depth of 22 mm and an open angle of 2° was added in the sugarcane model.

The front view and the top view of the simulation model are shown in Figure 21.

Moments and tested units are shown in Figure 22. Two tested units were chosen, unit 443386 and unit 440058, at the left side and the right side of the crack tip, respectively, to study how stresses at the crack tip change.

According to Figure 22(a), the tested unit, 443386, is the position which is closest to the initial cut-in point of the cutter while the tested unit, 440058, is the position which is the farthest from the initial cut-in point. That is, when the sugarcane is cut by the cutter, the cutter will cross the tested unit, 443386, firstly and then it will cross the tested unit, 440058, finally. When the sugarcane is cut from the left to the right, cutting forces will generate the torsional moment, T, and the bending moment, M, shown in Figure 22(b).

According to analysis on the high-speed photographing result in the sugarcane cutting process, there was an obvious height difference between the two cut-in points, so this simulation was designed as a single-factor experiment and the experimental factor is the cut-in height difference with four levels, 2 mm, 3 mm, 4 mm and 5 mm, to study how stresses along the x, the y, and the z axes near the crack tip change under actions of the torsional moment, the bending moment, and different cut-in height differences.

Curves of stresses of the two tested units along the x, the y, and the z axes change with time are shown in Figures 23 to 25.

According to Figure 23, the maximum value of x-directional stresses of the tested unit, 443386 appears earlier than that of the tested unit, 440058 and maximum values of x-directional stresses of these two tested units are both positive. The x axis is along the cut-in direction, so materials near the initial cut-in point have a trend to fall into the sugarcane while materials far away from the initial cut-in point have a trend to be separated from the sugarcane. Resistant forces against entering the sugarcane are greater than those against leaving the sugarcane. Therefore, cracks appear firstly in positions of the sugarcane far away from the initial cut-in point. x-directional stresses are generated by the bending moment shown in Figure 22(b).

According to Figure 24, the maximum value of y-directional stresses of the tested unit, 443386 appears earlier than that of the tested unit, 440058. The maximum value of y-directional stresses of the tested point, 443386 is positive while that of the tested unit, 440058 is negative, showing positions of the sugarcane near the initial cut-in point suffer from axial tensile forces while positions far away from the initial cut-in point suffer from axial pressures. y-directional stresses extend original cracks. Once y-directional stresses reach the axial tensile strength of the sugarcane, the sugarcane will be extended along the original crack direction.

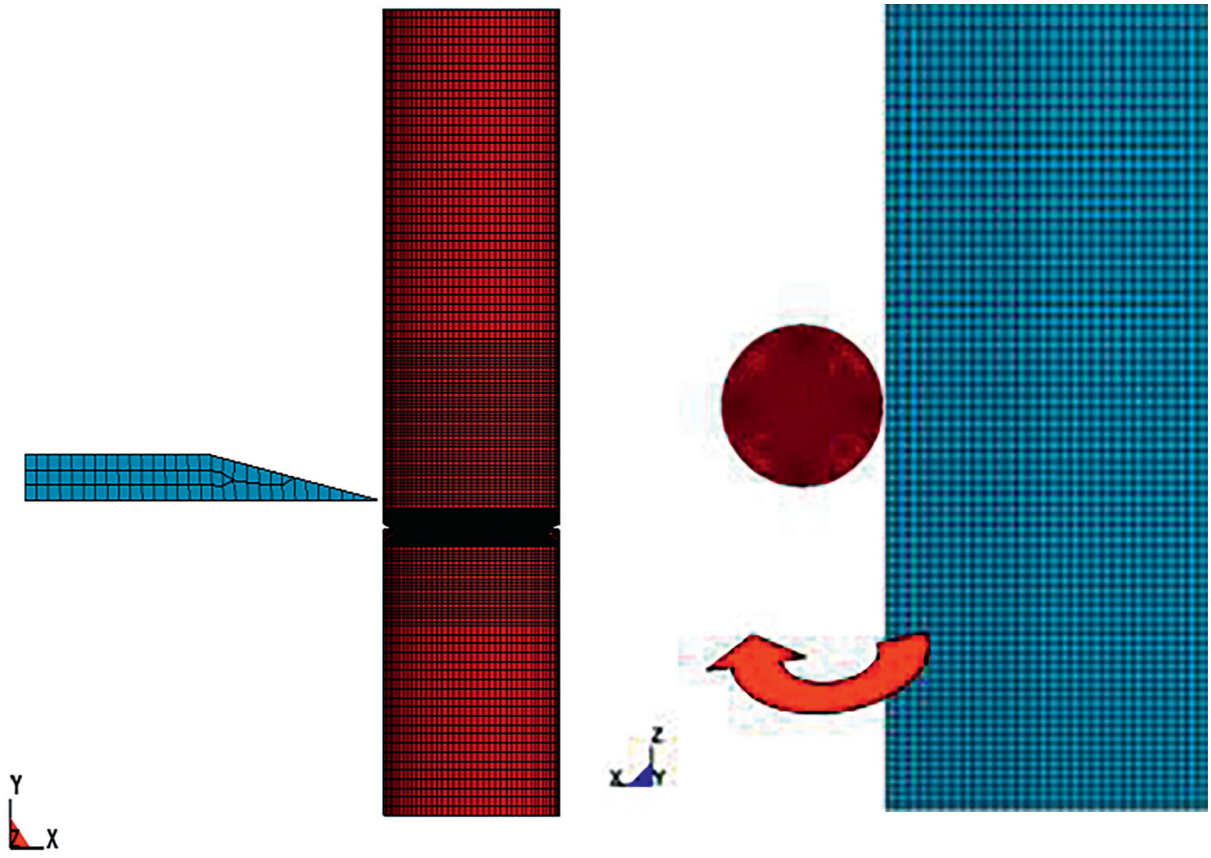

(a) (b)

Figure 21: The simulation model of a sugarcane cut along its side surface. (a) The front view of the simulation model. (b) The top view of the simulation model.

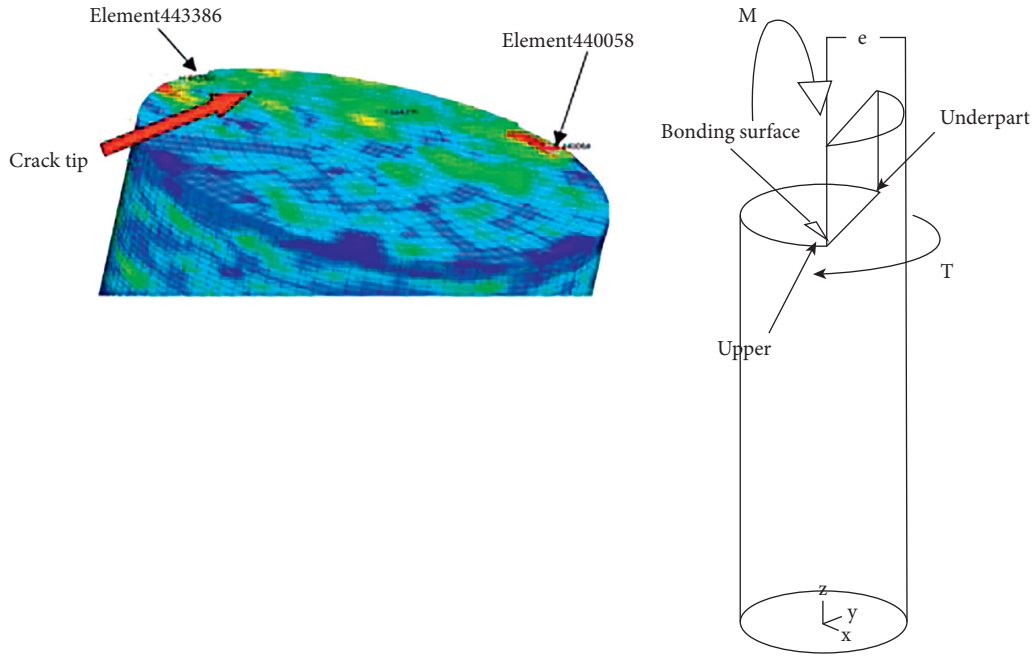

(a) (b)

Figure 22: Moments and tested units with the sugarcane set to be cut along its side surface. (a) Tested units. (b) The bending moment and the torsional moment.

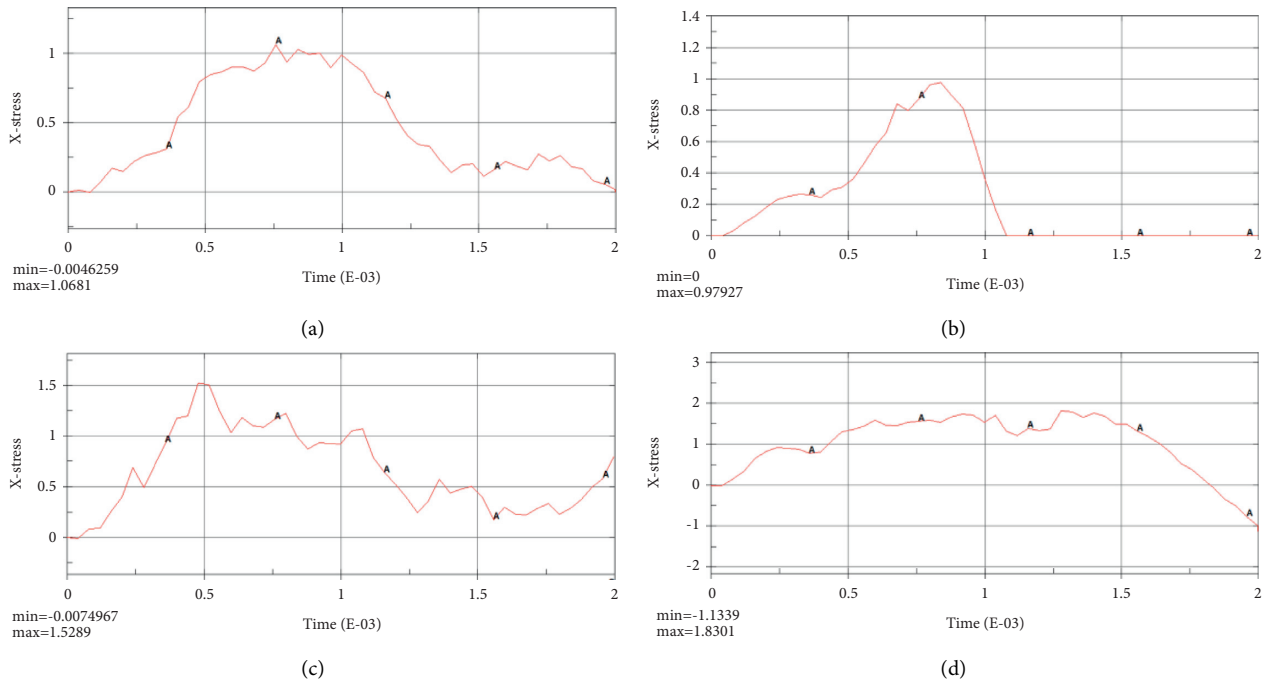

Figure 23: Curves of x-directional stresses of the two tested units changing with time under different cut-in heights. (a) The x-directional stress of the unit, 443386 under a cut-in height difference of 2 mm. (b) The x-directional stress of the unit, 440058 under a cut-in height difference of 2 mm. (c) The x-directional stress of the unit, 443386 under a cut-in height difference of 3 mm. (d) The x-directional stress of the unit, 440058 under a cut-in height difference of 3 mm.

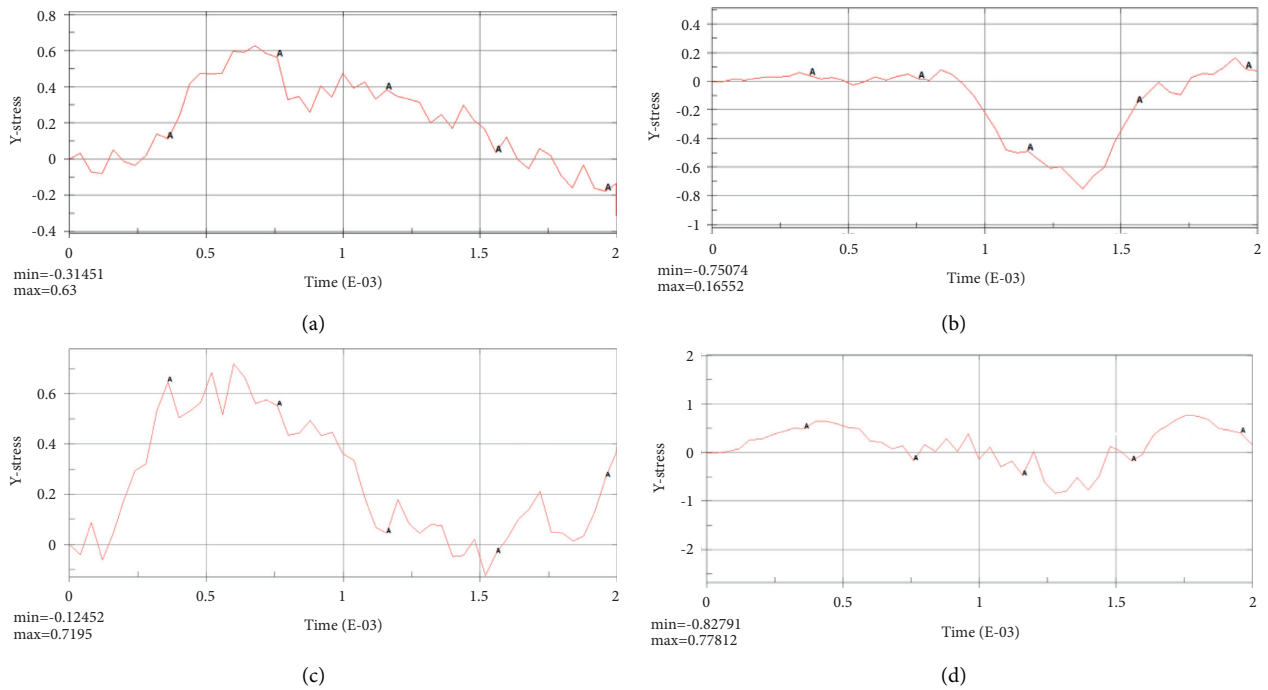

Figure 24: Curves of y-directional stresses of the two tested units changing with time under different cut-in heights. (a) The y-directional stress of the unit, 443386 under a cut-in height difference of 2 mm. (b) The y-directional stress of the unit, 440058 under a cut-in height of 2 mm. (c) The y-directional stress of the unit, 443386 under a cut-in height difference of 3 mm. (d) The y-directional stress of the unit, 440058 under a cut-in height difference of 3 mm.

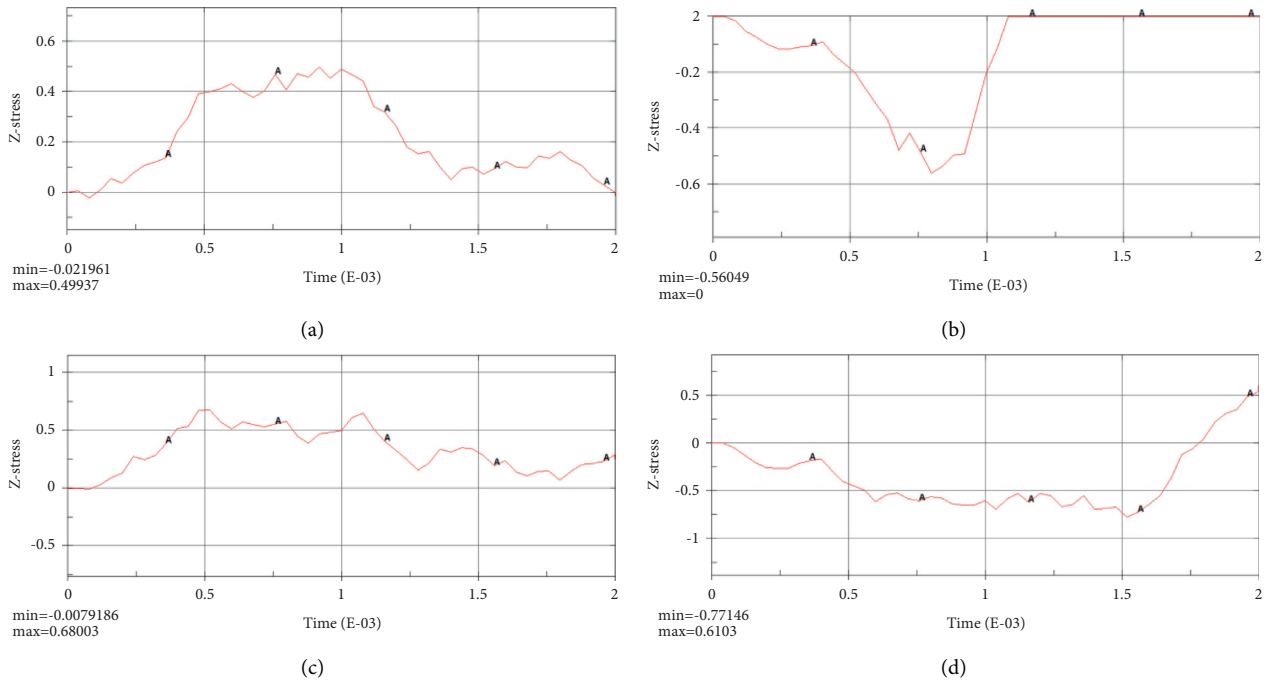

Figure 25: Curves of z-directional stresses of the two tested units changing with time under different cut-in height differences. (a) The z-directional stress of the unit, 443386 under a cut-in height difference of 2 mm. (b) The z-directional stress of the unit, 440058 under a cut-in height difference of 2 mm. (c) The z-directional stress of the unit, 443386 under a cut-in height difference of 3 mm. (d) The z-directional stress of the unit, 440058 under a cut-in height difference of 3 mm.

According to Figure 25, the maximum value of z-directional stresses of the tested unit, 443386 appears earlier than that of the tested unit, 440058. The maximum value of z-directional stresses of the tested point, 443386 is positive while that of the tested unit, 440058 is negative. This shows that not only will the sugarcane suffer from the action of the bending moment but will also suffer from the action of the torsional moment. Under the action of the torsional moment, z-directional stresses of positions of the sugarcane near the initial cut-in point are pressures making materials turn to the interior of the sugarcane. z-directional stresses of positions of the sugarcane far away from the initial cut-in point are tensions, making materials separated from the sugarcane, that is, breaking the surface of the sugarcane.

Maximum values of stresses of the two tested units along the x, the y, and the z axes are shown in Table 15to–17.

According to Table 15 and Figure 26(a), the greater the cut-in height difference, the greater the x-directional stresses will be. Fitting equations of x-directional stresses of the two tested units, 443386 and 440058 changing with the cut-in height difference are shown in

$$\sigma_{x_{44386}} = -0.045x^2 + 0.621x + 0.024, \quad (8)$$

$$\sigma_{x_{440058}} = -0.1975x^2 + 1.7475x - 1.7025. \quad (9)$$

Fitting curves of these three-directional stresses of the two tested units changing with the cut-in height difference are shown in Figure 26.

According to equations (8) and (9), there are quadratic relationships between x-directional stresses of the two tested units and the cut-in height difference. Determination coefficients of these two fitting equations are 0.9894 and 0.9878, showing that these fitting curves and their fitting equations have high fitting degrees.

According to Table 16 and Figure 26(b), the greater the cut-in height difference is, the greater the y-directional stresses will be. Fitting equations of y-directional stresses of the two tested units, 443386 and 440058 changing with the cut-in height difference are shown in

$$\sigma_{y_{443386}} = -0.0025x^2 + 0.1205x + 0.3945, \quad (10)$$

$$\sigma_{y_{440058}} = -0.0225x^2 + 0.0345x - 0.7295. \quad (11)$$

According to equations (10) and (11), there are linear relationships between y-directional stresses of the two tested units and the cut-in height difference. Determination coefficients of these two fitting equations are 0.9924 and 0.9999, showing that these fitting curves and their fitting equations have high fitting degrees.

According to Table 17 and Figure 26(c), the greater the cut-in height difference is, the greater the z-directional stresses will be. Fitting equations of z-directional stresses of the two tested units, 443386 and 440058 changing with the cut-in height difference are shown in

$$\sigma_{z_{443386}} = 0.01x^2 + 0.078x + 0.317, \quad (12)$$

$$\sigma_{z_{440058}} = 0.0125x^2 - 0.2425x - 0.1325. \quad (13)$$

According to equations (12) and (13), there are quadratic relationships between z-directional stresses of the two tested

Table 15: Maximum values of x-directional stresses under different cut-in height differences.

	σ_x (MPa)	
The cut-in height difference (mm)	The tested unit, 443386	The tested unit, 440058
2	1.07	0.98
3	1.53	1.83
4	1.74	2.06
5	2.02	2.12

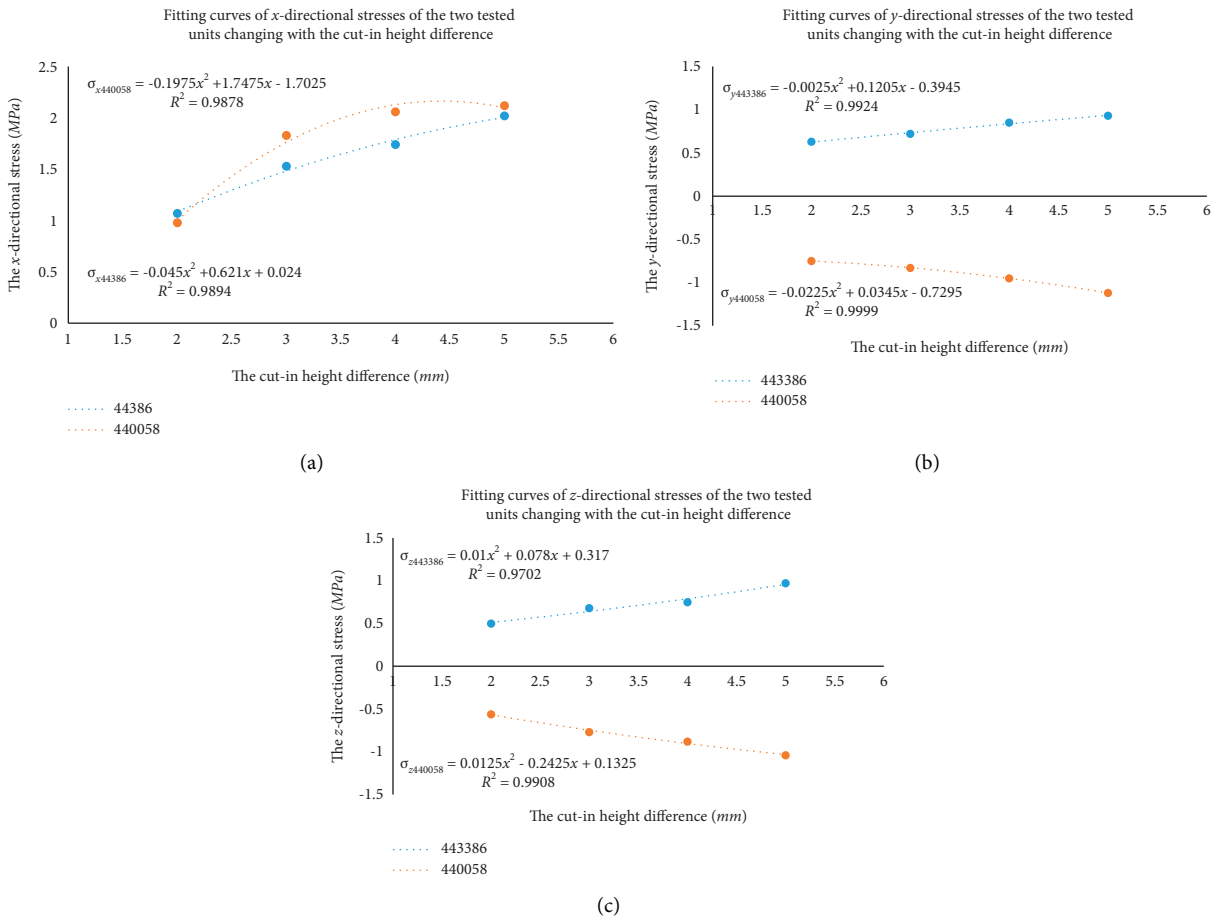

Figure 26: Fitting curves of these three-directional stresses of the two tested units changing with the cut-in height difference. (a) Fitting curves of x-directional stresses. (b) Fitting curves of y-directional stresses. (c) Fitting curves of z-directional stresses.

Table 16: Maximum values of y-directional stresses under different cut-in height differences.

	σ_y (MPa)	
The cut-in height difference (mm)	The tested unit, 443386	The tested unit, 440058
2	0.63	−0.75
3	0.72	−0.83
4	0.85	−0.95
5	0.93	−1.12

Table 17: Maximum values of z-directional stress under different cut-in height differences.

	σ_z (MPa)	
The cut-in height difference (mm)	The tested unit, 443386	The tested unit, 440058
2	0.5	−0.56
3	0.68	−0.77
4	0.75	−0.88
5	0.97	−1.04

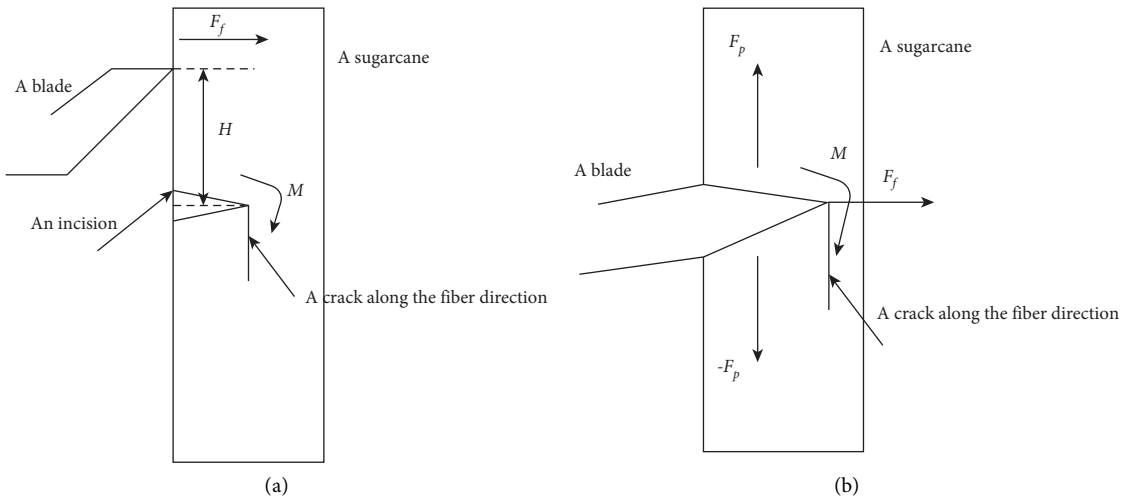

FIGURE 27: Force analysis of a sugarcane in the second cut with a lateral crack generated in the first cut. (a) The effect of the lateral force on the sugarcane. (b) The effect of the axial cutter vibration on the sugarcane.

units and the cut-in height difference. Determination coefficients of these two fitting equations are 0.9702 and 0.9908, showing that these fitting curves and their fitting equations have high fitting degrees.

According to analysis above, when a sugarcane with lateral cracks is cut on its lateral interface, three-directional stresses exist at the same time at both sides near and far away from the initial cut-in point because of a torsional moment and a bending moment, both acting on the sugarcane. The greater the cut-in height difference is, the greater the three-directional stresses will be. y-directional stresses extend cracks along their original directions. x and z-directional stresses tear the lateral interface of the sugarcane and generate axial cracks. Axial cracks usually appear at crack tips far away from the initial cut-in point firstly. Once axial cracks appear, the flexibility of the sugarcane will increase. As a result, small cutting forces can even extend these axial cracks only to break the sugarcane ratoon.

10. Analysis and Discussion

10.1. Effects of the Amplitude and the Frequency of the Axial Cutter Vibration on the CCQEV. According to analysis on cutting force signals, the high-speed photographing result, and simulation results, a sugarcane is cut off by the second or the third cut and a height difference exists between the two cut-in points, so force analysis of a sugarcane in the second cut with a lateral crack generated in the first cut is shown in Figure 27.

In the second cut, a lateral force, F_f acting on the sugarcane is generated by cutters. If the second cut-in point is higher than the first one, F_f will generate a bending moment, M at the first cut-in point. Sugarcanes are transversely isotropic materials with greater strength along the fiber direction than that along the lateral direction. Under the action of the bending moment, M, lateral cracks generated at the first cut-in point will be expanded along the sugarcane fiber direction as incisions shown in Figure 27(a), causing cracks along the sugarcane fiber direction and affecting the SCQ. The greater the axial cutter vibration amplitude is, the greater the cut-in height difference, H, will be, the greater the bending moment, M, will be, and the greater the rate of cracks along the sugarcane fiber direction will be, so the greater the axial cutter vibration amplitude is, the greater the CCQEV will be, that is, the poorer the SCQ will be.

According to Figure 27(b), because of the axial cutter vibration, an upward or a downward pressure will act on the sugarcane when blades move forward. Blades move forward and upward, generating an upward pressure, F_p, acting on the sugarcane. A forward force, F_f, will also act on the sugarcane when blades move forward. F_f and F_p are related to the friction coefficient, μ, between blades and the sugarcane. As is mentioned above, the greater F_p is, the greater F_f will be. F_f and F_p both act on the sugarcane, generating the bending moment, M, making sugarcane cracks along the fiber direction appear. The greater the axial cutter vibration frequency is, the greater F_p and F_f will be, the greater M will be, the more easily cracks along the sugarcane fiber direction will appear, so the greater the axial cutter vibration frequency is, the greater the CCQEV will be, that is, the poorer the SCQ will be.

When blades move forward and downward, a forward force, F_f, and a downward pressure, $-F_p$, will act on the sugarcane. The relationship between F_f and $-F_p$ is analogous to that between F_f and F_p, that is, the greater $-F_p$ is, the greater F_f will be. F_f will generate the bending moment, M, acting on the sugarcane. $-F_p$ presses the sugarcane. Under combined actions of M and $-F_p$, cracks will be generated along the sugarcane fiber direction. The greater the axial cutter vibration frequency is, the greater the bending moment, M, and the downward pressure, $-F_p$, will be, the more easily cracks along the sugarcane fiber direction will appear.

In conclusion, the greater the amplitude and the frequency of the axial cutter vibration are, the greater the CCQEV will be, that is, the poorer the SCQ will be, verifying

the interaction effect between the amplitude and the frequency of the axial cutter vibration on the CCQEV.

10.2. The Interaction Effect between the Axial Cutter Vibration Amplitude and the Cutter Rotation Velocity on the CCQEV. With the cutter rotation velocity increasing, it will take cutters less time to cut off a sugarcane. Under a constant axial cutter vibration amplitude, according to Figures 27(a) and 27(b), M increases enough to make cracks along the sugarcane fiber direction appear. If the sugarcane cutting time is less than the crack generating time, it will not be easy for cracks along the sugarcane fiber direction to appear, that is, the SCQ will be better.

11. Conclusions

(1) According to analysis on the orthogonal experiment result, significance levels of effects of five experimental factors on the CCQEV from high to low are as follows: the axial cutter vibration amplitude, the axial cutter vibration frequency, the sugarcane feeding velocity, the cutter rotation velocity, and the cutter installing angle.

(2) According to analysis on single-factor experiment results, the greater the amplitude and the frequency of the axial cutter vibration are, the greater the CCQEV will be, that is, the poorer the SCQ will be.

(3) According to value simulating calculation through MATLAB according to equation (4) obtained through the quadratic regressive orthogonal rotational experiment, the greater the cutter rotation velocity is, the smaller the CCQEV will be, that is, the better the SCQ will be while the greater the sugarcane feeding velocity is, the greater the CCQEV will be, that is, the poorer the SCQ will be. When the cutter installing angle is 5°, the CCQEV is the greatest, that is, the SCQ is the poorest.

(4) According to surface diagrams drawn through MATLAB according to equation (4), the interaction effect between the amplitude and the frequency of the axial cutter vibration on the CCQEV is that the greater the amplitude and the frequency of the axial cutter vibration are, the greater the CCQEV will be, that is, the poorer the SCQ will be. The interaction effect between the axial cutter vibration amplitude and the cutter rotation velocity on the CCQEV is the same.

(5) According to analysis on results of the orthogonal experiment, single-factor experiments, and the quadratic regressive orthogonal rotational experiment, for small sugarcane harvesters in hilly areas, the smaller the amplitude and the frequency of the axial cutter vibration are, the better the SCQ will be and best values of the cutter rotation velocity, the sugarcane feeding velocity, and the cutter installing angle are 750 RPM, 0.7 m/s and 15°.

(6) According to analysis on cutting force signals and the high-speed photographing result in the sugarcane cutting process, a sugarcane was cut off in several times of cutting and because of relative axial displacements between blades and sugarcanes caused by the axial cutter vibration, there was an obvious height difference between two cut-in points.

(7) According to analysis on the simulation result of the sugarcane cutting process without lateral sugarcane cracks under dynamic loads, the greater the axial cutter vibration amplitude is, the greater the resultant cutting force, F_f and F_p will be. According to analysis on the simulation result of the sugarcane cutting process with lateral sugarcane cracks under dynamic loads, the greater the cut-in height difference is, the greater the three-directional stresses will be.

(8) Analysis on cutting force signals, the high-speed photographing result, and simulation results verified effects of the amplitude and the frequency of the axial cutter vibration, their interaction effect, and the interaction effect between the axial cutter vibration amplitude and the cutter rotation velocity on the CCQEV.

(9) This research laid the development foundation of small sugarcane harvesters with a good SCQ in hilly areas.

Data Availability

All data, models, and codes generated and used during this study are available from the first author by request.

Conflicts of Interest

The authors declare that there are no conflicts of interest regarding the publication of this paper.

Authors' Contributions

Prof. Shangping Li, Dr. Jinghui Zhou, Dr. Chen Qiu, and Hanning Mo discussed the idea and finally determined the title of this manuscript after Hanning Mo put forward the topic. Guiqing He, Bang Zeng, and Hanning Mo designed experiments under Prof. Shangping Li's guidance. Guiqing He, Bang Zeng, and Hanning Mo designed, manufactured, and adjusted the sugarcane harvester experiment platform. Prof. Shangping Li funded it. Guiqing He, Bang Zeng, Dr. Chen Qiu, and Dr. Jinghui Zhou helped Hanning Mo carry out experiments. Guiqing He and Bang Zeng helped Hanning Mo analyze experiment results and process the data. Hanning Mo wrote this manuscript, Prof. Shangping Li and Dr. Chen Qiu reviewed it, and Hanning Mo revised it according to their comments several times. All the authors agreed on what this manuscript is presented like finally.

Acknowledgments

This paper with its relevant work was supported by a National Natural Science Foundation Project (China) called Research on Critical Technologies and Mechanisms of

Continuous Precise Planting for Transversal Double-Bud Sugarcane Planters (Grant Number: 52165009), 2021, a Middle-Aged and Young Teachers' Basic Scientific Research Ability Promotion Project of Guangxi Universities (China) called Dynamic Reverse Design Research on Sugarcane Harvesters for Hilly Areas Based on Dynamic Characteristics of Cutters (Project number: 2020KY17008), 2020, a Key University-Level Scientific Research Project of Wuzhou University (China) called Reverse Design Method Research on Sugarcane Harvesters for Hilly Areas Based on Dynamic Characteristics of Cutters (Project Number: 2020B003), 2020, a National Natural Science Foundation Project (China) called Research on Cutting System Vibration Characteristics of Sugarcane Harvesters under Complicated Excitations (Grant Number: 51465006), 2014, and a Key Manufacturing System and Advanced Manufacture Laboratory Project of Guangxi (China) (Project Number: 14-045-15S01).

References

[1] Q. Fan, Q. Huang, and H. Wu, "Prospect and development of sugarcane mechanized harvest at home and abroad," *Sugarcane and Canesugar*, vol. 49, no. 6, pp. 1–11, 2020.

[2] S. Kroes and H. D. Harris, "Variation of cutting energies along a sugarcane internode," in *Proceedings of the Conference on Engineering in Agriculture and Food Processing*, vol. 25, no. 3, p. 55, Queensland, Australia, 1996.

[3] S. Kroes and H. D. Harris, "The specific splitting energy of sugarcane," in *Proceedings of the 1998 Conference of the Australian Society of Sugar Cane Technologists held at Ballina*, pp. 349–356, Ballina, Australia, May 1998.

[4] C. M. Roberto da and H. D. Harris, "Cane damage and mass losses for conventional and serrated hasecutter blades," *Proceedings of the Australian Society of Sugar Cane Technologists*, vol. 22, pp. 84–91, 2000.

[5] S. Kroes and H. D. Harris, "Effects of cane harvester base cutter parameters on the quality of cut," *Proceedings of the Australian Society of Sugar Cane Technologists*, pp. 169–179, 1994.

[6] R. D. C. Mello and H. Harris, "Desempenho de cortadores de base para colhedoras de cana-de-açúcar com lâminas serrilhadas e inclinadas," *Revista Brasileira de Engenharia Agrícola e Ambiental*, vol. 7, no. 2, pp. 355–358, 2003.

[7] Q. Liu, Y. Ou, S. Qing, and C. Song, "Mechanics analysis on stubble damage of sugarcane stalk during cutting by smooth-edge blade," *Transactions of the Chinese Society for Agricultural Machinery*, vol. 38, no. 9, pp. 70–73, 2007.

[8] Q. Liu, Y. Ou, and S. Qing, "Stubble damage of sugarcane stalks in cutting experiment by smooth-edge blade," *Transactions of the Chinese Society for Agricultural Machinery*, vol. 23, no. 3, pp. 103–107, 2007.

[9] Q. Liu, Y. Ou, and S. Qing, "Study on the cutting mechanism of sugarcane stem," *Journal of Agricultural Mechanization Research*, no. 1, pp. 21–24, 2007.

[10] J. Yang and G. Chen, "Experimental study on influencing factors of broken biennial root rate for a single base cutter of sugarcane harvester," *Transactions of the Chinese Society for Agricultural Machinery*, vol. 38, no. 3, pp. 69–74, 2007.

[11] Y. Wang, J. Yang, and Z. Liu, "Dynamic simulation experiment on effects of sugarcane cutting beneath surface soil," *Transactions of the Chinese Society of Agricultural Engineering*, vol. 27, no. 8, pp. 150–157, 2011.

[12] S. Thanomputra and T. Kiatiwat, "Simulation study of cutting sugarcane using fine sand abrasive waterjet," *Agriculture and Natural Resources*, vol. 50, no. 2, 2016.

[13] R. da Cunha Mello and H. D. Harris, "Angle and serrated blades reduce damage, force and energy for a harvester basecutter," *Proceedings of the Australian Society of Sugar Cane Technologists*, vol. 23, pp. 212–218, 2001.

[14] M. A. Momin, P. A. Wempe, T. E. Grift, and A. C. Hansen, "Effects of four base cutter blade designs on sugarcane stem cut quality," *Transactions of the ASABE*, vol. 60, no. 5, pp. 1551–1560, 2017.

[15] T. C. Ripoli and M. L. C. Ripoli, "Effects of two different base cutters in green cane mechanical harvest," *International Annual Meeting*, ASAE Riviera Hotel and Convention Center, no. 7, , pp. 27–30, Las Vegas, NV, USA, 2003.

[16] P. C. Johnson, C. L. Clementson, S. K. Mathanker, T. E. Grift, and A. C. Hansen, "Cutting energy characteristics of Miscanthus x giganteus stems with varying oblique angle and cutting speed," *Biosystems Engineering*, vol. 112, no. 1, pp. 42–48, 2012.

[17] S. K. Mathanker, T. E. Grift, and A. C. Hansen, "Effect of blade oblique angle and cutting speed on cutting energy for energycane stems," *Biosystems Engineering*, vol. 133, pp. 64–70, 2015.

[18] S. Kroes and H. D. Harris, "A kinematic model of the dual basecutter of a sugar cane harvester," *Journal of Agricultural Engineering Research*, vol. 62, no. 3, pp. 163–172, 1995.

[19] S. Kroes and H. D. Harris, *Cutting Forces and Energy during an Impact Cut of Sugarcane Stalks*, pp. 1–8, EurAgEng'96 Madrid, Tanikon, Switzerland, 1996.

[20] R. P. D. Silva, C. F. Corrêa, J. W. Cortez, and C. E. A. Furlani, "Controle estatístico aplicado ao processo de colheita mecanizada de cana-de-açúcar," *Engenharia Agrícola*, vol. 28, no. 2, pp. 292–304, 2008.

[21] L. Xiao, S. Li, and F. Ma, "Effect of field excitation on cutting quality for sugarcane," *Transactions of the Chinese Society for Agricultural Machinery*, vol. 42, no. 12, pp. 97–101, 2011.

[22] X. Lai, S. Li, and F. Ma, "Simulation and experimental study on sugarcane field excitation to the cutter," *Advanced Materials Research*, vol. 156-157, p. 1035, 2011.

[23] P. Wang and D. Wei, "Research on the influence of bearing clearance on vibration characteristics of sugarcane cutter," *Agricultural Equipment & Vehicle Engineering*, vol. 51, no. 7, pp. 6–9, 2013.

[24] H. Huang, Y. Wang, and Y. Tang, "Finite element simulation of sugarcane cutting," *Transactions of the Chinese Society of Agricultural Engineering*, vol. 27, no. 2, pp. 161–166, 2011.

[25] Q. Liu, Y. Ou, and S. Qing, "Cutting force calculation of sugarcane stalk," *Transactions of the Chinese Society for Agricultural Machinery*, vol. 37, no. 9, pp. 89–92, 2006.

[26] X. Xu, Z. Yin, and X. Sun, "Finite element simulation of reciprocating sugarcane cutter," *Value Engineering*, vol. 37, no. 1, pp. 148–150, 2018.

[27] J. Yang, Z. Liang, and J. Mo, "Experimental research on factors affecting the cutting quality of sugarcane cutter," *Transactions of the Chinese Society of Agricultural Engineering*, vol. 21, no. 5, pp. 60–64, 2005.

[28] M. F. Pelloso, B. F. Pelloso, A. A. De Lima, and A. H. Tiene Ortiz, "Influence of harvester and rotation of the primary extractor speed in the agroindustrial performance of sugarcane," *Sugar Tech*, 2021.

[29] Z. Cheng, *Structure Design snd Analysis and Experiment Research of the Carrying Frame in Minitype Sugarcane Harvester*, Master Thesis, Guangxi University, Nanning, China, 2007.

[30] J. Zhou, S. Li, D. Yang, and J. Zhong, "Influence of sugarcane harvester cutterhead axial vibration on the sugarcane ratoon cutting quality," *Transactions of the Chinese Society of Agricultural Engineering*, vol. 33, no. 2, pp. 16–24, 2017.

[31] F. Ma, Y. He, and S. Li, "Analysis on fuzzy comprehensive evaluation and optimization of cutting performance of sugarcane harvester," *Transactions of the Chinese Society for Agricultural Machinery*, vol. 37, no. 12, 2006.

[32] J. Zhou, *Research on the Influences of Axial Vibration of Sugarcane Harvester Cutting Systems on Sugarcane Cutting Quality*, Doctoral Thesis, Guangxi University, Nanning, China, 2017.